



HAL
open science

The decisive role of pericyclic reactions in the thermal decomposition of organophosphorus compounds

J.-C. Lizardo-Huerta, B. Sirjean, L. Verdier, R Fournet, Pierre-Alexandre Glaude

► **To cite this version:**

J.-C. Lizardo-Huerta, B. Sirjean, L. Verdier, R Fournet, Pierre-Alexandre Glaude. The decisive role of pericyclic reactions in the thermal decomposition of organophosphorus compounds. Proceedings of the Combustion Institute, 2021, 38 (1), pp.719-727. 10.1016/j.proci.2020.08.007 . hal-03195795

HAL Id: hal-03195795

<https://hal.science/hal-03195795>

Submitted on 12 Apr 2021

HAL is a multi-disciplinary open access archive for the deposit and dissemination of scientific research documents, whether they are published or not. The documents may come from teaching and research institutions in France or abroad, or from public or private research centers.

L'archive ouverte pluridisciplinaire **HAL**, est destinée au dépôt et à la diffusion de documents scientifiques de niveau recherche, publiés ou non, émanant des établissements d'enseignement et de recherche français ou étrangers, des laboratoires publics ou privés.

**The decisive role of pericyclic reactions in the thermal decomposition of
organophosphorus compounds**

J.-C. Lizardo-Huerta¹, B. Sirjean¹, L. Verdier², R. Fournet¹, P.-A. Glaude¹

¹ Laboratoire Réactions et Génie des Procédés, CNRS, Université de Lorraine

1 rue Grandville BP 20451 54001 Nancy Cedex, France

² DGA Maîtrise NRBC, Site du Bouchet, 5 rue Lavoisier, BP n°3, 91710 Vert le Petit, France

Corresponding author :

Pierre-Alexandre Glaude

Laboratoire Réactions et Génie des Procédés

1 rue Grandville BP 20451 54001 Nancy Cedex,

France

Email: pierre-alexandre.glaude@univ-lorraine.fr

Abstract

The understanding of the thermal decomposition chemistry of chemical warfare nerve agents is largely limited by the scarcity of kinetic data. Because of the high toxicity of these molecules, experimental determination of their chemical properties is very difficult. In the present work, a comprehensive detailed kinetic model for the decomposition of sarin and some simulants, i.e. di-isopropyl methyl phosphonate (DIMP), diethyl methylphosphonate (DEMP), and triethyl phosphate (TEP) were developed, containing possible molecular and radical pathways. The importance of unimolecular pericyclic decomposition led to evaluate precisely the rate constants of these reactions with high level theoretical calculations. The QCISD(T)/cc-PV ∞ QZ//B2PLYPD3/6-311+G(2d,d,p) level of theory was selected after a benchmark. The contribution of hindered rotors was included with the 1D-HR-U approach. Tunneling was taken into account for H-atom transfer. Transition state theory was used to calculate high-pressure limit rate constants and pressure dependent rate constants were calculated using Master Equation modelling. The model was validated against experimental pyrolysis and oxidation experimental data available in literature. Flux analyses showed that whatever the conditions are, the first step of decomposition of the studied phosphorus compounds are pericyclic eliminations leading to successive decompositions, whereas bond-breaking or H-atom abstraction remain negligible, even at high temperature.

Keywords

Organophosphorus compounds, chemical warfare agents, sarin, DIMP, DEMP, TEP, modeling, theoretical chemistry

Introduction

Organophosphorus compounds are involved in many toxics such as pesticides (i.e. malathion) or in chemical warfare nerve agents such as sarin. Although these compounds have a relatively long lifetime at room temperature [1], their high temperature behaviour is not well known. Fighting fires in pesticide stockpiles or dimensioning processes for the thermal destruction of nerve agents requires a good knowledge of the reactivity and distribution of products. Despite their high toxicity, few experimental studies have been performed for the destruction of chemical warfare agents [2,3]. Incineration [4,5] belongs to the most widespread methods of destruction envisaged. However, the main studies have been carried out with simulants of nerve agents, as dimethyl methylphosphonate (DMMP), diethyl methylphosphonate (DEMP), di-isopropyl methyl phosphonate (DIMP), triethyl phosphate (TEP). These molecules are less toxic but do not contain the heteroatoms involved in real compounds, such as fluorine in sarin.

In pyrolysis, Durig *et al.* [6] studied reactions of six organophosphorus compounds, including DMMP, and proposed a decomposition pathway based on unimolecular eliminations. Zegers and Fisher investigated the thermal decomposition of DIMP [7], DEMP [8] and TEP [9] in the range of 700-900 K. They proposed a reaction scheme based on some successive pericyclic molecular eliminations. Some experimental studies in the literature investigated the inhibiting effect of nontoxic organophosphorus compounds as fire retardant in flames [10]. Korobeinichev *et al.* investigated the decomposition of several organophosphorus compounds such as DIMP in H₂/O₂/Ar premixed flames [11]. They quantified phosphorous oxides using molecular beam mass spectrometry with tuneable electron-impact ionization. Glaude *et al.*

[12,13] have modelled the combustion of sarin, DMMP and DIMP. They pointed out the important role of molecular elimination reactions even in highly reactive combustion conditions and showed that DMMP, which cannot react through a six-membered elimination, was not a suitable surrogate for sarin, contrary to DIMP. In shock tube, Mathieu *et al.* [14] investigated the influence of DMMP on hydrogen, methane, and ethylene ignition in shock tube and Neupane *et al.* studied experimentally [15] and modelled [16] the decomposition of TEP.

Quantum chemical calculations have been used to determine mainly thermochemical properties [17,18], but also rate constants of molecular systems containing trivalent or pentavalent phosphorus [19]. Sullivan *et al.* [20] investigated the combustion of methylphosphonic acid (MPA) at the CBS-Q level of theory and evaluated several elementary reactions, such as the unimolecular decomposition of MPA and the hydrogen abstraction from MPA by OH radicals. Comparison with literature showed significant discrepancies especially for reactions involving P-O bonds and highlighted the fact that reaction rates based on analogous C-O bond chemistry are unreliable. More recently, a theoretical investigation of unimolecular decomposition of DMMP was reported by Yang *et al.* [21]. The most favourable elimination through a 4-membered transition state yields methanol and $\text{O}=\text{P}(\text{CH}_2)(\text{OCH}_3)$ and involves a barrier of $73.2 \text{ kcal mol}^{-1}$ at the CBS-QB3 level of theory. These calculations are supported by the experimental investigation of the thermal decomposition of DMMP probed by VUV synchrotron radiation and photoelectron photoion coincidence spectroscopy [22], which showed that DMMP decomposes by successive losses of methanol and formaldehyde yielding CH_3PO , which eventually produces PO and methyl radicals. Unimolecular decomposition of sarin and soman have been investigated systematically at the CBS-QB3 level of theory by Ash *et al.* [23], showing the prominent role of the 6-membered ester elimination of propene over other pericyclic reactions, with an energy barrier around 40

kcal mol⁻¹ much lower than in the case of DMMP. Shan *et al.* [24] evaluated the 6-centered pericyclic reaction of sarin with high level methods. The rate constant reproduced very well experimental measurements of sarin decomposition over a temperature range 350-500 °C.

These results show that unimolecular reactions could play a major role in the thermal decomposition of organophosphorus compounds. The present study aims to propose a comprehensive detailed kinetic model of the pyrolysis and combustion of sarin and its surrogates, i.e. DIMP, DEMP and TEP (Figure 1), containing both molecular and radical chain reactions. to unravel the relative importance of the pericyclic mechanisms over a wide range of pressure and temperature. The selection of the computational method to calculate theoretically molecular pericyclic reactions is discussed first. A second part details the potential energy surface for the molecular eliminations of the studied compounds and the calculation of rate constants. The detailed model is then presented and validated against experimental data from the literature.

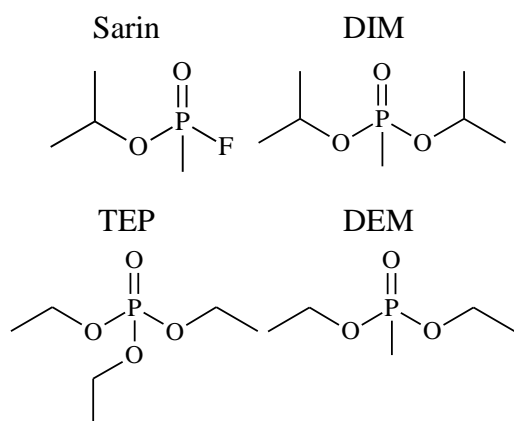


Figure 1: Structure of sarin and its surrogates

Quantum chemical calculation methodology

All *ab initio* calculations have been performed using Gaussian 09 suite of quantum chemistry program [25]. Before choosing the correct method for calculating the electronic structure, we performed a benchmark of composite methods, such as CBS-QB3, G4, as well as CCSD(T)/cc-PV ∞ QZ//B2PLYPD3/6-311+G(2d,d,p) and QCISD(T)/cc-

PV ∞ QZ//B2PLYPD3/6-311+G(2d,d,p), these last methods being inspired from the work of Goldsmith *et al.* [26], using the more powerful double-hybrid density functional method B2PLYPD3 for geometry optimizations, which has shown a good ability for reducing the geometric and ZPE uncertainties [27]. Energies at the QCISD(T)/cc-pVDZ and QCISD(T)/cc-pVTZ levels of theory were calculated with the DFT geometries. The complete basis set (CBS) limit energy was then calculated from the extrapolations of the cc-pVDZ and cc-pVTZ results. Extrapolations from the triple and quadruple- ζ basis set calculations have been tested for light species but are prohibitive for molecules of interest. Eventually the MP2 method was used to correct for the difference in the TZ and DZ basis sets based extrapolations [26]:

$$\begin{aligned}
 E_{QCISD(t)/\infty(Q)Z} &= E_{QCISD(t)/TZ} + \left(E_{QCISD(t)/TZ} - E_{QCISD(t)/DZ} \right) \frac{3^4}{4^4 - 3^4} \\
 &+ E_{MP2/QZ} + \left(E_{MP2/QZ} - E_{MP2/TZ} \right) \frac{4^4}{5^4 - 4^4} \\
 &- E_{MP2/TZ} - \left(E_{MP2/TZ} - E_{MP2/DZ} \right) \frac{3^4}{4^4 - 3^4} \quad (1)
 \end{aligned}$$

In order to compare the methods, calculations of thermochemical data have been performed on organophosphorus species for which the thermodynamic data are well known. The results are presented in Table S1. These results agree with the experimental data whatever the method, with mean standard deviations from experiments around 3 kcal mol⁻¹ in enthalpies. In the case of sarin, for which experimental data are not available, high level methods differ widely from the popular CBS-QB3 method. For all species involved in calculations, enthalpies of formation ($\Delta_f H_{298K}^\circ$) were estimated from the electronic energies using atomisation energies, excepted for hydrocarbons, for which experimental data have been used. The reference data for atoms are derived from NIST database [28].

To increase precision, the low-frequency modes of vibration corresponding to internal rotations have been treated as hindered rotors rather than harmonic oscillators. The energy barriers were calculated with the levels of theory previously described, while the internal rotor

processing was carried out using the 1-DHR-U method [29]. Classical Transition State Theory (TST) was used to deduce rate constants from the energy of reactants, transition states and products. The tunnelling effect was taken into account for reactions involving an internal H-transfer by employing the Eckart method [30]. The kinetic parameters were fitted using the three parameters modified Arrhenius equation ($A \times T^n \times \exp(-E_a/RT)$) over the temperature range 300–2000 K. The calculation of the kinetic and thermodynamic parameters, following this methodology, was carried out using the THERMROT software [31]. This software, developed in our laboratory, makes it possible to easily retrieve the relevant data from Gaussian calculation files and to calculate the kinetic parameter as well as thermodynamic data in the form of NASA polynomials. Influence of pressure was evaluated using master equation (ME) modelling with the MESS code [32]. Rate constants at different pressure have been calculated in nitrogen as a bath gas. Details of the parameters used in the resolution of the ME can be found in Table S2.

Choice of method

The various methods previously described have been tested for the calculation of kinetic data in order to draw the best option. The molecular elimination reactions of sarin and its decomposition product, respectively TS1 and TS2 in Figure 2, have been used as a test case. Note that the initial decomposition of sarin involves two transition states (TS1-1 and TS2), related to the relative position of the non-reactive methyl group and F-atom, as mentioned by Shan *et al.* [24]. Energy barriers obtained at 0 K are presented in Table 1. The structure of TS1-1, TS1-2 and TS2 is displayed in figure S1.

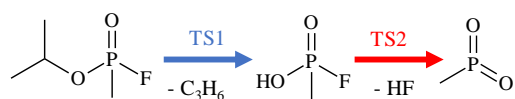


Figure 2: Molecular decomposition of sarin, showing six-membered (blue) and four-membered (red) elimination reactions.

Table 1: Molecular decomposition of sarin: energy barriers at 0 K computed at different level of theory.

	CBS- QB3	G4	CCSD(T)/ $\infty(Q)Z$	QCISD(T)/ $\infty(Q)Z$
TS1-1	40.0	39.5	38.9	38.5
TS1-2	40.2	39.7	39.2	38.7
TS2	51.4	51.5	51.5	51.1

Subsequently, the kinetic constants obtained with the different methods were included in the detailed kinetic model of the thermal decomposition of sarin. The Senkin program of Chemkin II [33] was used to simulate the decomposition of sarin under pyrolysis. The simulations were done for temperatures ranging from 350 to 500 °C, the initial pressure was set at 1 bar, and the residence time ran up to 0.5 s, at the experimental conditions carried out by Shan *et al.* [24]. The results obtained are presented in Figure 3. It can be observed that the rate constants obtained at the QCISD(T)/cc-PV ∞ QZ//B2PLYPD3/6-311+G(2d,d,p) level of theory are those that show the best agreement with the experimental results. This method will then be adopted for further calculations.

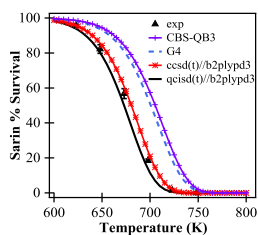


Figure 3: Comparison at different levels of calculation of the evolution of sarin decomposition as a function of temperature. Initial pressure, 1 bar; residence time, 0.5 s. Symbols, experimental results [24]; lines, simulations.

Kinetic Modelling

A detailed chemical kinetic model has been developed to simulate the pyrolysis and combustion of sarin and its simulants. The structure and the name of reactant and specific products are displayed in Figure S2 in the Supplemental Material. The mechanism has been written in a comprehensive way, and includes both molecular and radical mechanisms. The model consists in four parts: (1) a C/H/O reaction base from our laboratory [34]; (2) a phosphorus reaction base from LLNL mechanisms for nerve agents surrogates [35]; (3) a sub-mechanism of sarin and DIMP from Glaude *et al.* [13] updated in this work; (4) a molecular decomposition mechanism of DEMP and TEP developed in this work.

The first part (1) includes all the reactions involving radicals or molecules containing less than three carbon atoms, coupled with a reaction base for C₃-C₄ multi-unsaturated hydrocarbons [34,36]. Pressure-dependent rate constants and efficiency coefficients are included. Thermochemical data were taken from literature or computed software THERGAS based on group additivity [37]. The kinetic data were taken from the literature, or estimated from quantitative structure-reactivity relationships. The second part (2) consists in the

reaction base for phosphorus oxides from LLNL validated against TMP and DMMP reactions in flames [35].

The third part (3) contains the mechanisms for the degradation of sarin and DIMP. The primary mechanism was systematically built using generic rules of radical chain reactions [38], which represents all the possible reactions for the reactant and the radicals produced. Sub-mechanisms have been written in the same way for the reactions of the molecular products. Thermochemical data have been calculated theoretically for all the stable species and the free radicals produced, as well as the kinetic parameters of the molecular pericyclic reactions. Unimolecular initiations have been written in the reverse way as radical combinations and their rate constants were estimated by analogy with that of hydrocarbon radicals [39]. Parameters for the addition of OH on the P=O bond and those for internal isomerization have been estimated with the correlation used for the alkenes [38]. Addition of H-atom on the P=O bond has been neglected [35]. Rate parameters of radical decomposition by β -scission have been calculated theoretically with the methodology described above when the broken bond involves the P-atom. Reactions of alkyl chains were estimated by analogy with reactions of alkanes [38]. Rate constants of H-atom abstractions on the alkyl chain by H, OH and CH₃ have been evaluated using an Evans–Polanyi correlation proposed for hydrocarbons [40]. The fourth part (4) includes the molecular mechanism of the degradation of DEMP and TEP and their primary products. Molecular decompositions were calculated theoretically as that of sarin and DIMP. These pericyclic reactions consist of concerted six-centered and four-centered cyclic complexes as shown in Figure 2 for sarin and in Figure 4 for the simulants. Thermodynamic and kinetic parameters were calculated theoretically with the methods described above. The kinetic parameters were calculated for the high-pressure limit and for the low-pressure dependence from 0.01 to 100 atm. Note that the Master Equation calculations were computed together for the different unimolecular reactions

involved in each reaction scheme. All the data are displayed in the Table S3. A sub-mechanism has been added for ethanol [41], which is formed during the decomposition of DEMP and TEP, to update the C₀-C₂ reaction base [34].

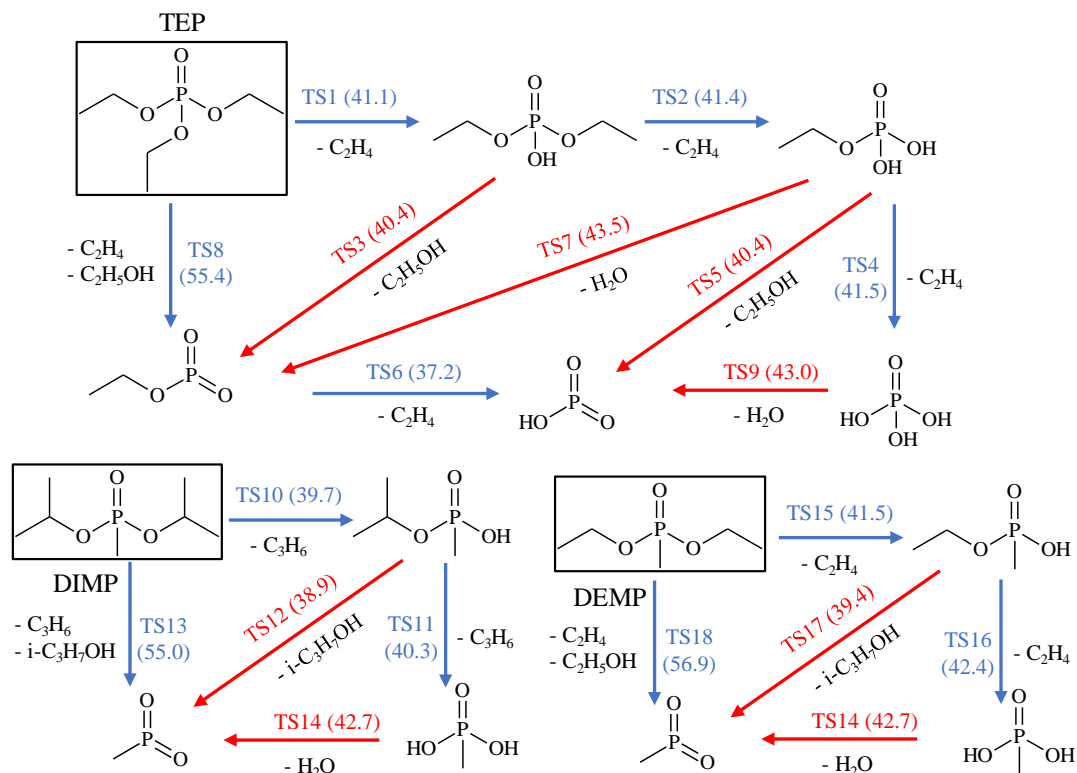


Figure 4: Molecular decomposition of sarin simulants (TEP, DIMP and DEMP), showing six-centered (blue) and four-centered (red) pericyclic reactions with their respective energy barriers at 0 K, computed at the QCISD(T)/cc-PV ∞ QZ//B2PLYPD3/6-311+G(2d,d,p) level of theory and including ZPE (in kcal mol⁻¹).

The final mechanisms were written in the format of CHEMKIN II [33]. The mechanism of sarin involves 226 species reacting in 1343 reactions, that of DIMP, DEMP and TEP (in one model), 313 species in 2048 reactions. The mechanisms are available among the Supplementary Materials.

Results and discussion

The kinetic models were used to simulate the thermal behavior of sarin and its simulants and compare with available experimental data. Simulations were performed with the software SENKIN from CHEMKIN II [33].

Sarin pyrolysis was simulated at the conditions of Shan et al. [24], as shown in Figure 5. Figure 5 displays the percentage of remaining sarin as a function of temperature at various residence times. These results show a very good agreement with the experimental results, which ensures the quality of the methodology retained in this work. It confirms also that the thermal decomposition of this type of species occurs by a molecular decomposition mechanism, as already discussed in the literature [13,23,24].

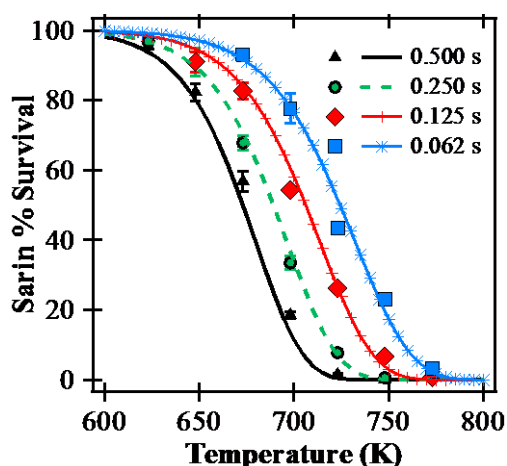


Figure 5: Evolution of sarin decomposition as a function of residence time and temperatures using the comprehensive mechanism including the kinetic constants calculated at the QCISD(T)/cc-PV ∞ QZ//B2PLYPD3/6-311+G(2d,d,p) level of theory. Symbols: experiments [24]; lines, simulations.

The decomposition of the simulants were simulated at the conditions of Zegers and co-workers [7–9]. Experiments were conducted in a quartz-lined turbulent flow reactor with nitrogen as carrier gas, the pressure was kept at 1 atm for temperatures between 700 and 900 K. The initial compositions were 115 ppm for DIMP; 36 and 60 ppm for DEMP and 31 and 124 ppm for TEP. The decomposition products, as well as the reactants, were analysed by

FTIR, these products were: isopropanol and propene in the case of DIMP, while ethanol and ethylene in the cases of DEMP and TEP. Simulations reproduce the experiments at high working temperatures (Figure 6). In the case of lower temperatures, some discrepancies appear between simulations and experiences, which may be due to a deposition or a reaction of the reactants at the reactor walls, as mentioned by the authors. Such a heterogeneous effect should have a larger influence at lower temperature. For instance, in the case of TEP pyrolysis, the very high amount of ethylene observed at 802K does not really match with TEP conversion and ethanol formation.

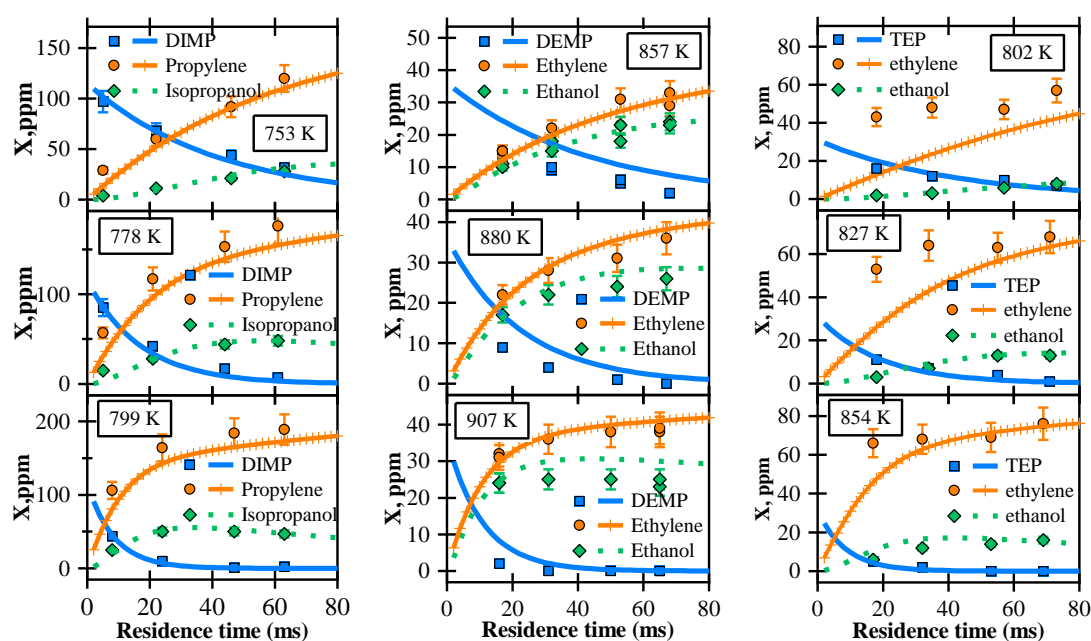


Figure 6: Mole fraction of the simulant and their respective alcohol and alkene formed during their thermal decomposition at various residence time and temperatures. Initial pressure, 1 atm; initial mole fraction of DIMP, 115 ppm; DEMP, 36 ppm and TEP, 31 ppm. Symbols, experimental results: DIMP [7], DEMP [8] and TEP [9] ; lines, simulation.

At higher temperatures, the primary decomposition products, such as ethylene and ethanol, also react. Figures 7 compares the CO yields obtained during the reaction of TEP in shock tube, in pyrolysis (Fig. 6a-c) and oxidation (Fig. 6d-g) respectively, by Neupane *et al.* [15] and simulations carried out with the model from these authors [16] and our model.

Experimental uncertainty in the measured CO mole fraction was estimated to be 7.2% or ± 123 ppm [15]. The results show that both models follow the same behaviour in pyrolysis and oxidation. In pyrolysis, the increasing amount of CO with temperature indicate a change in the ratio between ethylene and ethanol formation during TEP decomposition (see Figure 4), ethanol being the source of CO in pyrolysis. Sensitivity analyses show that in pyrolysis the most promoting reaction for CO formation is the decomposition of TEP into $C_2H_5OPO_2$ and ethanol, whereas the competing reaction of decomposition into diethylphosphate and ethylene inhibits the most the production of CO. Note that the radical mechanism does not play any role in the decomposition of TEP and intermediates until decomposition of ethylene and ethanol. The better agreement of our model at the highest temperature may come from the increasing importance of the pressure effect on molecular decomposition of TEP and intermediates, which is included in our model.

In combustion, the model is able to predict both CO profile shape and maximum amount. An underestimation is observed at short residence times at the lowest temperature, whereas the decay of CO for longer residence times is underestimated at 1437K. Sensitivity and flow analyses show that in combustion, the reactions of CO are linked to the hydrocarbon mechanism and to its interactions with phosphorus oxide reaction bases, which need certainly to be improved. The most promoting reactions for the formation of CO are reactions of oxidation of ethylene with O atoms and OH radicals.

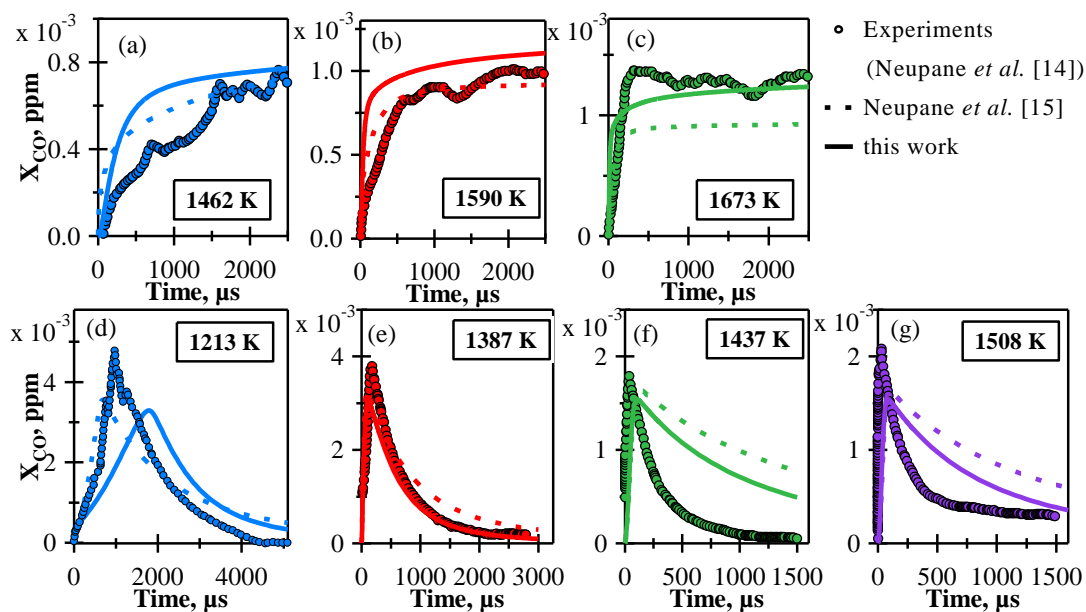


Figure 7: CO time history during TEP pyrolysis (a-c) and oxidation (d-g). Pyrolysis: (a, b, c) $X_{\text{TEP}} = 0.25\%$ in Ar, $P = 1.3\text{--}1.4$ atm. Combustion: (d, e) $X_{\text{TEP}} = 0.076\%$, $\phi = 0.075$, bath gas Ar, $P = 1.42\text{--}1.32$ atm, (f, g) $X_{\text{TEP}} = 0.038\%$, $\phi = 0.078$, $P = 1.27\text{--}1.17$ atm. Symbols, experimental results [15]; simulations, this work (solid curve), literature model [16] (dashed curve).

Figure 8 compares the conversion of sarin and its surrogates in a close vessel at the conditions of Figure 4. It appears that the decomposition of sarin is the fastest whereas DEMP is the less reactive simulant. DIMP appears to be the best surrogate for sarin among these species since it shows a close reactivity and similar hydrocarbon products, i.e. propene. An interesting point is that at all conditions, radical reactions remains negligible in the conversion of the organophosphorus reactant and of the intermediates described in Figure 3. A flux analysis performed for sarin in presented in Figure S3. Whatever the temperature is, sarin decomposes by the loss of propene followed by the elimination of HF, producing CH_3PO_2 , which eventually breaks into a methyl radical and PO_2 and initiates radical reactions. The final decomposition products of sarin and its surrogates, which do not contain phosphorus, are propene and isopropyl alcohol in the case of sarin and DIMP, ethylene and ethanol in the

cases of DEMP and TEP. These products react then in radical reactions. Whatever the conditions are, even when the pool of radicals due to the combustion of hydrocarbon and alcohol increases, the organophosphorus species decompose only by the low barrier pericyclic reactions. H-atom abstractions remain always negligible in sarin consumption, and account for only 1% of the flux at 2000K. Same conclusions can be done for DIMP, DEMP and TEP.

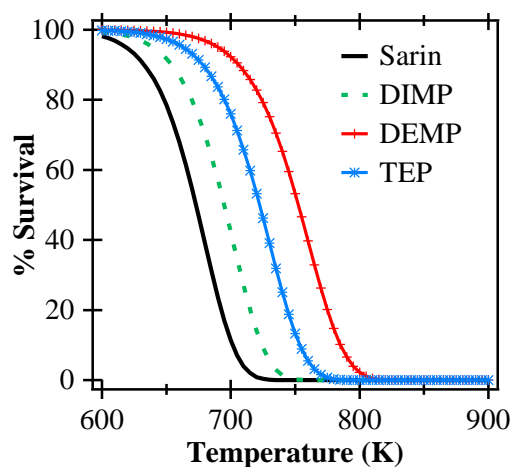


Figure 8: Conversion of sarin and its simulants vs. temperatures in pyrolysis in a closed vessel. Initial pressure, 1 bar; residence time, 0.5 s.

Conclusions

The effect of molecular decomposition reactions on thermal degradation of organophosphorus species is investigated. High level theoretical calculations of the pericyclic rate constants have been performed with an original methodology, taking into account the tunnel effect, the effect of the pressure and an exhaustive treatment of internal rotations both in the reagents and in the transition states. Comprehensive detailed mechanisms were developed for the thermal decomposition and combustion of sarin, DIMP, DEMP, and TEP which includes radical chain reactions and all the molecular pericyclic reactions. Simulations and comparisons with the experimental results of the literature show that our model predicts correctly the thermal decomposition and the combustion of sarin and its simulants. It appears that these species decompose uniquely through the pericyclic reactions, until species without P-atom are produced. The models can then be drastically reduced to keep only these unimolecular decompositions in the primary mechanisms of organophosphorus reactants, while more complex radical reactions concern small phosphorus oxides, and hydrocarbon and alcohol products. Further improvements of the model would then focus on the phosphorus reaction base and its connexion with hydrocarbon reactions.

Acknowledgements

This work was supported by DGA Maîtrise NRBC. High performance computing resources were provided by the EXPLOR centre hosted by the University of Lorraine. and IDRIS under the allocation 2018-A0010807249 made by GENCI.

References

- [1] P. Martin, E.C. Tuazon, R. Atkinson, A.D. Maughan, Atmospheric Gas-Phase Reactions of Selected Phosphorus-Containing Compounds, *J. Phys. Chem. A.* 106 (2002) 1542–1550. <https://doi.org/10.1021/jp012720d>.
- [2] Y.C. Yang, J.A. Baker, J.R. Ward, Decontamination of chemical warfare agents, *Chem. Rev.* 92 (1992) 1729–1743. <https://doi.org/10.1021/cr00016a003>.

- [3] R.S. Thompson, M.R. Brann, E.H. Purdy, J.D. Graham, A.A. McMillan, S.J. Sibener, Rapid Laser-Induced Temperature Jump Decomposition of the Nerve Agent Simulant Diisopropyl Methylphosphonate under Atmospheric Conditions, *J. Phys. Chem. C*. 123 (2019) 21564–21570. <https://doi.org/10.1021/acs.jpcc.9b05381>.
- [4] J.F. Bunnett, M. Mikolajczyk, *Arsenic and Old Mustard: Chemical problems in the destruction of old arsenical and mustard munitions*, Kluwer Academic Publishers, 1998.
- [5] O.P. Korobeinichev, V.M. Shvartsberg, A.G. Shmakov, Destruction of organophosphorus compounds in flames and nonthermal plasmas, *Russ. J. Phys. Chem. B*. 2 (2008) 856–875. <https://doi.org/10.1134/S1990793108060031>.
- [6] J.R. Durig, D.F. Smith, D.A. Barron, Thermal decomposition studies of some organophosphorus compounds, *Journal of Analytical and Applied Pyrolysis*. 16 (1989) 37–48. [https://doi.org/10.1016/0165-2370\(89\)80034-8](https://doi.org/10.1016/0165-2370(89)80034-8).
- [7] E.J.P. Zegers, E.M. Fisher, Gas-Phase Pyrolysis of Diisopropyl Methylphosphonate, *Combustion and Flame*. 115 (1998) 230–240. [https://doi.org/10.1016/S0010-2180\(98\)00003-0](https://doi.org/10.1016/S0010-2180(98)00003-0).
- [8] E.J.P. Zegers, E.M. Fisher, Gas-Phase Pyrolysis of Diethyl Methylphosphonate, *Combustion Science and Technology*. 116–117 (1996) 69–89. <https://doi.org/10.1080/00102209608935544>.
- [9] E.J.P. Zegers, E.M. Fisher, Pyrolysis of Triethyl Phosphate, *Combustion Science and Technology*. 138 (1998) 85–103. <https://doi.org/10.1080/00102209808952064>.
- [10] V.M. Shvartsberg, T.A. Bolshova, O.P. Korobeinichev, Effect of Iron and Organophosphorus Flame Inhibitors on the Heat Release Rate in Hydrogen/Oxygen Flames at Low Pressure, *Energy Fuels*. 25 (2011) 596–601. <https://doi.org/10.1021/ef1014814>.
- [11] O.P. Korobeinichev, A.A. Chernov, T.A. Bolshova, The chemistry of the destruction of organophosphorus compounds in flames—IV: destruction of DIMP in a flame of H₂ + O₂ + Ar, *Combustion and Flame*. 123 (2000) 412–420. [https://doi.org/10.1016/S0010-2180\(00\)00141-3](https://doi.org/10.1016/S0010-2180(00)00141-3).
- [12] P.A. Glaude, H.J. Curran, W.J. Pitz, C.K. Westbrook, Kinetic study of the combustion of organophosphorus compounds, *Proceedings of the Combustion Institute*. 28 (2000) 1749–1756.
- [13] P.A. Glaude, C. Melius, W.J. Pitz, C.K. Westbrook, Detailed chemical kinetic reaction mechanisms for incineration of organophosphorus and fluoroorganophosphorus compounds, *Proceedings of the Combustion Institute*. 29 (2002) 2469–2476.
- [14] O. Mathieu, W.D. Kulatilaka, E.L. Petersen, Experimental and modeling study on the effects of dimethyl methylphosphonate (DMMP) addition on H₂, CH₄, and C₂H₄ ignition, *Combustion and Flame*. 191 (2018) 320–334. <https://doi.org/10.1016/j.combustflame.2018.01.020>.
- [15] S. Neupane, F. Barnes, S. Barak, E. Ninnemann, Z. Loparo, A.E. Masunov, S.S. Vasu, Shock Tube/Laser Absorption and Kinetic Modeling Study of Triethyl Phosphate Combustion, *J. Phys. Chem. A*. 122 (2018) 3829–3836. <https://doi.org/10.1021/acs.jpca.8b00800>.
- [16] S. Neupane, R.K. Rahman, A.E. Masunov, S.S. Vasu, Theoretical Calculation of Reaction Rates and Combustion Kinetic Modeling Study of Triethyl Phosphate (TEP), *J. Phys. Chem. A*. 123 (2019) 4764–4775.

- [17] A. Khalfa, M. Ferrari, R. Fournet, B. Sirjean, L. Verdier, P.A. Glaude, Quantum Chemical Study of the Thermochemical Properties of Organophosphorous Compounds, *J. Phys. Chem. A.* 119 (2015) 10527–10539. <https://doi.org/10.1021/acs.jpca.5b07071>.
- [18] A. Burcat, The ideal gas thermochemistry of inorganic and organic phosphorous compounds and their ions, *Combustion and Flame.* 182 (2017) 238–247. <https://doi.org/10.1016/j.combustflame.2017.04.023>.
- [19] D.K. Hahn, K.S. Raghuveer, J.V. Ortiz, Computational Tests of Models for Kinetic Parameters of Unimolecular Reactions of Organophosphorus and Organosulfur Compounds, *J. Phys. Chem. A.* 115 (2011) 14143–14152. <https://doi.org/10.1021/jp206344r>.
- [20] P.A. Sullivan, R. Sumathi, W.H. Green, J.W. Tester, Ab initio modeling of organophosphorus combustion chemistry, *Phys. Chem. Chem. Phys.* 6 (2004) 4296–4309. <https://doi.org/10.1039/B402742F>.
- [21] L. Yang, R.M. Shroll, J. Zhang, U. Lourderaj, W.L. Hase, Theoretical Investigation of Mechanisms for the Gas-Phase Unimolecular Decomposition of DMMP, *J. Phys. Chem. A.* 113 (2009) 13762–13771. <https://doi.org/10.1021/jp904232n>.
- [22] S. Liang, P. Hemberger, N.M. Neisius, A. Bodi, H. Grützmacher, J. Levalois-Grützmacher, S. Gaan, Elucidating the Thermal Decomposition of Dimethyl Methylphosphonate by Vacuum Ultraviolet (VUV) Photoionization: Pathways to the PO Radical, a Key Species in Flame-Retardant Mechanisms, *Chem. Eur. J.* 21 (2015) 1073–1080. <https://doi.org/10.1002/chem.201404271>.
- [23] T. Ash, T. Debnath, T. Banu, A.K. Das, Exploration of Unimolecular Gas-Phase Detoxication Pathways of Sarin and Soman: A Computational Study from the Perspective of Reaction Energetics and Kinetics, *Chem. Res. Toxicol.* 29 (2016) 1439–1457. <https://doi.org/10.1021/acs.chemrestox.6b00132>.
- [24] X. Shan, J.C. Vincent, S. Kirkpatrick, M.D. Walker, M.R. Sambrook, D.C. Clary, A Combined Theoretical and Experimental Study of Sarin (GB) Decomposition at High Temperatures, *The Journal of Physical Chemistry A.* 121 (2017) 6200–6210. <https://doi.org/10.1021/acs.jpca.7b04282>.
- [25] M. Frisch, G. Trucks, H. Schlegel, G. Scuseria, M. Robb, J. Cheeseman, G. Scalmani, V. Barone, B. Mennucci, G. Petersson, H. Nakatsuji, M. Caricato, X. Li, H. Hratchian, A. Izmaylov, J. Bloino, G. Zheng, J. Sonnenberg, M. Hada, M. Ehara, K. Toyota, R. Fukuda, J. Hasegawa, M. Ishida, T. Nakajima, Y. Honda, O. Kitao, H. Nakai, T. Vreven, J. Montgomery, J. Peralta, F. Ogliaro, M. Bearpark, J. Heyd, E. Brothers, K. Kudin, V. Staroverov, R. Kobayashi, J. Normand, K. Raghavachari, A. Rendell, J. Burant, S. Iyengar, J. Tomasi, M. Cossi, N. Rega, J. Millam, M. Klene, J. Knox, J. Cross, V. Bakken, C. Adamo, J. Jaramillo, R. Gomperts, R. Stratmann, O. Yazyev, A. Austin, R. Cammi, C. Pomelli, J. Ochterski, R. Martin, K. Morokuma, V. Zakrzewski, G. Voth, P. Salvador, J. Dannenberg, S. Dapprich, A. Daniels, Farkas, J. Foresman, J. Ortiz, J. Cioslowski, D. Fox, Gaussian 09, Revision D.01, (2009).
- [26] C.F. Goldsmith, G.R. Magoon, W.H. Green, Database of Small Molecule Thermochemistry for Combustion, *J. Phys. Chem. A.* 116 (2012) 9033–9057. <https://doi.org/10.1021/jp303819e>.
- [27] L. Goerigk, S. Grimme, A thorough benchmark of density functional methods for general main group thermochemistry, kinetics, and noncovalent interactions, *Phys. Chem. Chem. Phys.* 13 (2011) 6670. <https://doi.org/10.1039/c0cp02984j>.
- [28] W. Mallard, P. Lindstrom, NIST Chemistry WebBook, NIST Standard Reference Database Number 69, 2016.

- [29] P. Vansteenkiste, D.V. Neck, V.V. Speybroeck, M. Waroquier, An extended hindered-rotor model with incorporation of Coriolis and vibrational-rotational coupling for calculating partition functions and derived quantities, *The Journal of Chemical Physics*. 124 (2006) 044314.
- [30] C. Eckart, The Penetration of a Potential Barrier by Electrons, *Phys. Rev.* 35 (1930) 1303–1309.
- [31] J.-C. Lizardo-Huerta, B. Sirjean, R. Bounaceur, R. Fournet, Intramolecular effects on the kinetics of unimolecular reactions of β -HORO \dot{O} and HOQ \dot{O} OOH radicals, *Phys. Chem. Chem. Phys.* 18 (2016) 12231–12251.
- [32] Y. Georgievskii, J.A. Miller, M.P. Burke, S.J. Klippenstein, Reformulation and Solution of the Master Equation for Multiple-Well Chemical Reactions, *J. Phys. Chem. A*. 117 (2013) 12146–12154. <https://doi.org/10.1021/jp4060704>.
- [33] R.J. Kee, F.M. Rupley, J.A. Miller, CHEMKIN II. A Fortran Chemical Kinetics Package for the Analysis of Gas-Phase Chemical Kinetics, Sandia Laboratories Report, SAND 89-8009B, 1993. <http://www.osti.gov/scitech/biblio/5681118> (accessed April 19, 2017).
- [34] E. Pousse, Z.Y. Tian, P.A. Glaude, R. Fournet, F. Battin-Leclerc, A lean methane premixed laminar flame doped with components of diesel fuel part III: Indane and comparison between n-butylbenzene, n-propylcyclohexane and indane, *Combustion and Flame*. 157 (2010) 1236–1260.
- [35] T.M. Jayaweera, C.F. Melius, W.J. Pitz, C.K. Westbrook, O.P. Korobeinichev, V.M. Shvartsberg, A.G. Shmakov, I.V. Rybitskaya, H.J. Curran, Flame inhibition by phosphorus-containing compounds over a range of equivalence ratios, *Combustion and Flame*. 140 (2005) 103–115. <https://doi.org/10.1016/j.combustflame.2004.11.001>.
- [36] N. Belmekki, P.A. Glaude, I. Da Costa, R. Fournet, F. Battin-Leclerc, Experimental and modeling study of the oxidation of 1-butyne and 2-butyne, *Int. J. Chem. Kinet.* 34 (2002) 172–183. <https://doi.org/10.1002/kin.10035>.
- [37] C. Muller, V. Michel, G. Scacchi, G.M. Côme, Thergas - a Computer-Program for the Evaluation of Thermochemical Data of Molecules and Free-Radicals in the Gas-Phase, *J Chim Phys.* 92 (1995) 1154–1178.
- [38] F. Buda, R. Bounaceur, V. Warth, P.A. Glaude, R. Fournet, F. Battin-Leclerc, Progress toward a unified detailed kinetic model for the autoignition of alkanes from C4 to C10 between 600 and 1200 K, *Combustion and Flame*. 142 (2005) 170–186.
- [39] D.L. Allara, R. Shaw, A compilation of kinetic parameters for the thermal degradation of n-alkane molecules, *Journal of Physical and Chemical Reference Data*. 9 (1980) 523–560. <https://doi.org/10.1063/1.555623>.
- [40] A.M. Dean, J.W. Bozzelli, Combustion chemistry of nitrogen, in: *Gas-Phase Combustion Chemistry*, Springer, 2000: pp. 125–341. http://link.springer.com/chapter/10.1007/978-1-4612-1310-9_2 (accessed February 1, 2017).
- [41] L.-S. Tran, P.-A. Glaude, R. Fournet, F. Battin-Leclerc, Experimental and Modeling Study of Premixed Laminar Flames of Ethanol and Methane, *Energy Fuels*. 27 (2013) 2226–2245.

Supplemental Material

File ESI_sarin-simulants

Figure S1: Geometry of TS1-1, TS1-2 and TS2 in the decomposition of sarin

Figure S2: Geometry of sarin, simulants and products.

Figure S3: Flux analysis for the thermal decomposition of sarin in nitrogen in an isothermal close reactor.

Table S1: Thermodynamic data calculated using the various methods and compared with experimental data.

Table S2: Parameters used in the master equation simulation of the molecular decomposition of sarin and their simulants.

Table S3: High-pressure limit (k_{∞}) and dependent pressure rate constants calculated for the molecular decomposition of sarin and its simulants calculated using the QCISD(T)/cc-PV ∞ QZ//B2PLYPD3/6-311+G(2d,d,p) level of theory.

Table S4: Optimized geometries (Cartesian coordinates) at the QCISD(T)/cc-PV ∞ QZ//B2PLYPD3/6-311+G(2d,d,p) level of theory of the species and transition states (TS) from Table S3.

Mechanism file:

Sarin_lrgp-0120

Sarin-simulalants_lrgp-0120

Supplemental Information

The decisive role of pericyclic reactions in the thermal decomposition of organophosphorous compounds

J.-C. Lizardo-Huerta¹, B. Sirjean¹, L. Verdier², R. Fournet¹, P.-A. Glaude¹

¹ Laboratoire Réactions et Génie des Procédés, CNRS, Université de Lorraine

1 rue Grandville BP 20451 54001 Nancy Cedex, France

² DGA Maîtrise NRBC, Site du Bouchet, 5 rue Lavoisier, BP n°3, 91710 Vert le Petit, France

Figure S1: Geometry of TS1-1, TS1-2 and TS2 in the decomposition of sarin

Figure S2: Geometry of sarin, simulants and products.

Figure S3: Flux analysis for the thermal decomposition of sarin in nitrogen in an isothermal close reactor.

Table S1: Thermodynamic data calculated using the various methods and compared with experimental data.

Table S2: Parameters used in the master equation simulation of the molecular decomposition of sarin and their simulants.

Table S3: High-pressure limit (k_{∞}) and dependent pressure rate constants calculated for the molecular decomposition of sarin and its simulants calculated using the QCISD(T)/cc-PV ∞ QZ//B2PLYPD3/6-311+G(2d,d,p) level of theory.

Table S4: Optimized geometries (Cartesian coordinates), electronic energies at 0 K and ZPE (in hartree) at the QCISD(T)/cc-PV ∞ QZ//B2PLYPD3/6-311+G(2d,d,p) level of theory of the species and transition states (TS) from Table S3.

Figure S1: Geometry of TS1-1, TS1-2 and TS2 in the decomposition of sarin

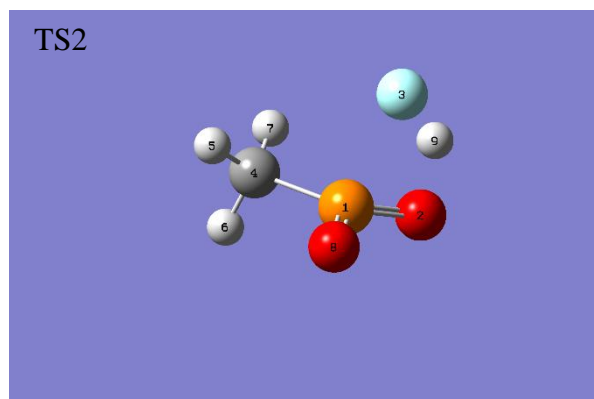
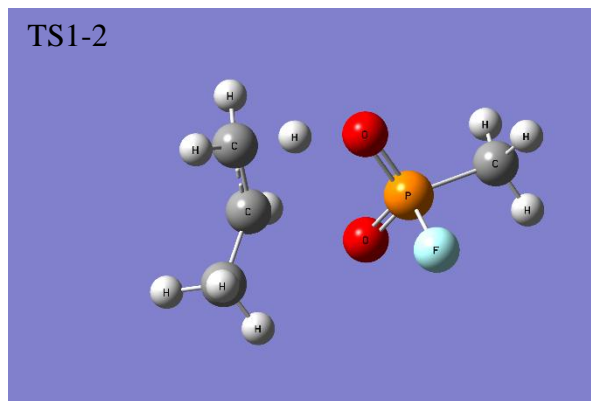
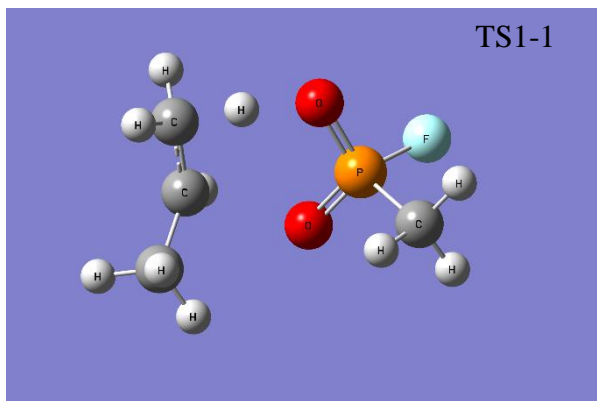


Figure S2: Geometry of sarin, simulants and products.

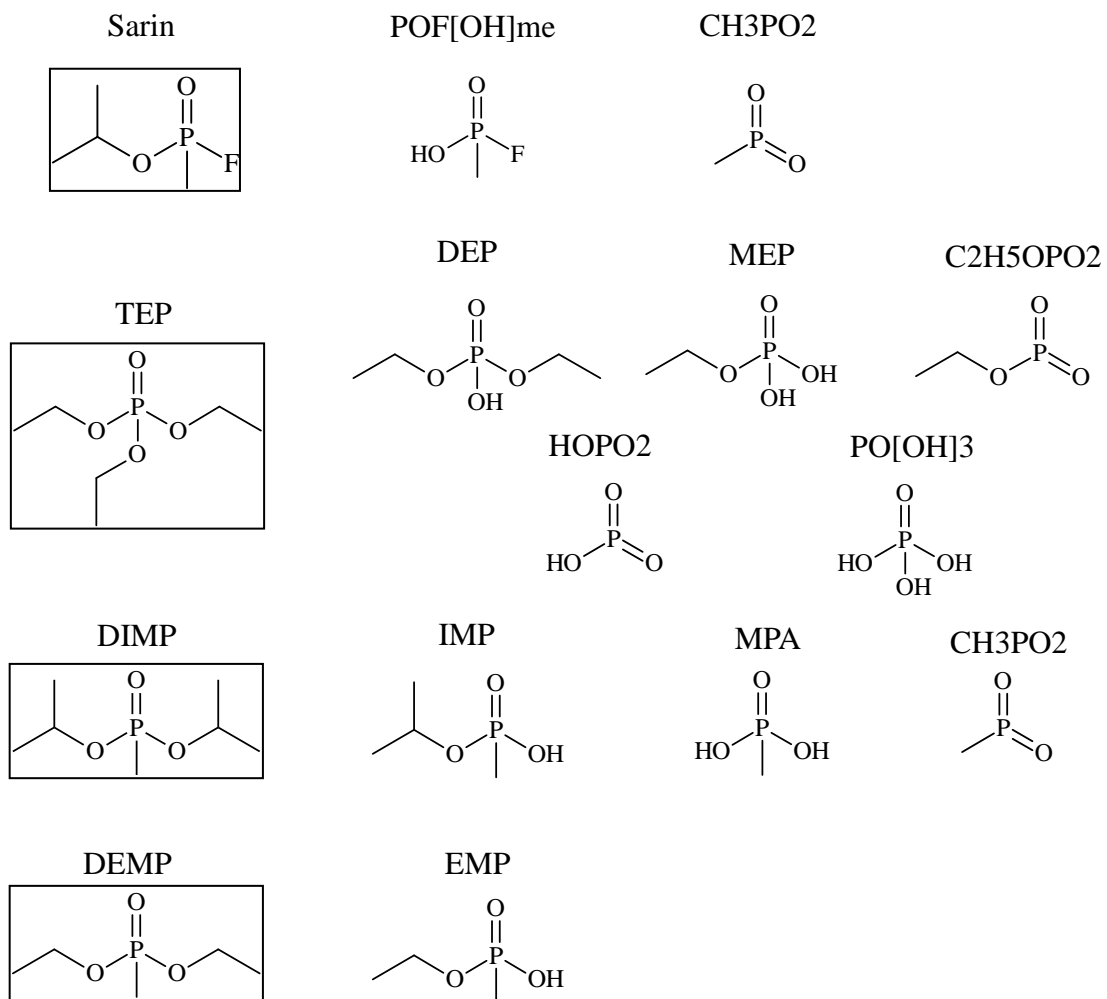


Figure S3: Flux analysis for the thermal decomposition of sarin in nitrogen in an isothermal close reactor under atmospheric pressure for residence time 1 ms.

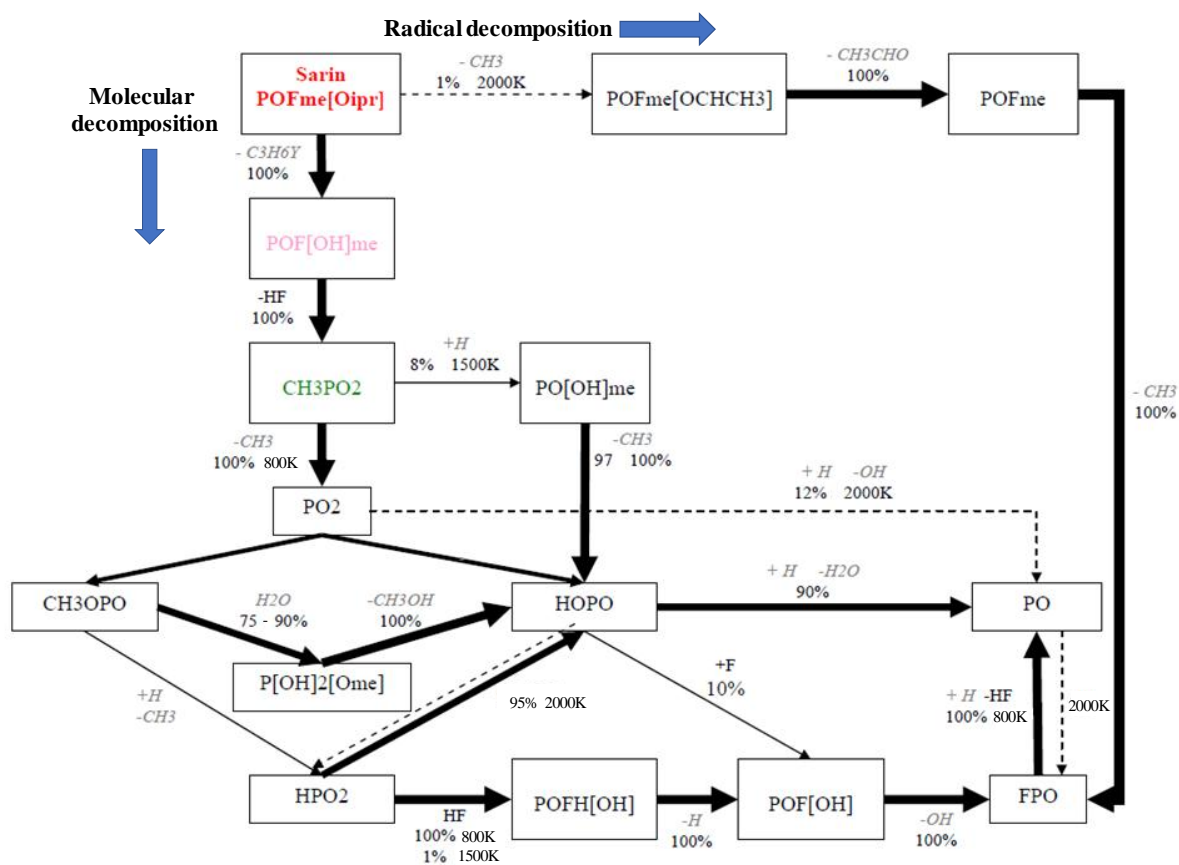


Table S1: Thermodynamic data calculated using the various methods and compared with experimental data.

	Exp. (NIST)	CBS- QB3	G4	ccsd(t)- mp2 ^a	qcisd(t)- mp2 ^b	ccsd(t) ^c	qcisd(t) ^d
PH₃							
ΔH_f° (kcal/mol)	1.29	0.42	2.8	1.38	1.31	1.55	1.49
S° (cal/mol K)	50.25	50.20	50.21	50.16	50.16	50.16	50.16
C_p° (cal/mol K)	8.87	8.80	8.80	8.75	8.75	8.75	8.75
PO							
ΔH_f° (kcal/mol)	-6.66	-8.21	-9.3	-3.08	-3.72	-5.63	-6.35
S° (cal/mol K)	53.24	52.09	52.10	52.12	52.12	52.12	52.12
C_p° (cal/mol K)	7.59	7.13	7.124	7.165	7.165	7.165	7.165
PO₂							
ΔH_f° (kcal/mol)	-67.29	-70.97	-67.4	-66.92	-68.34	-67.27	-68.56
S° (cal/mol K)	60.63	60.86	60.87	60.86	60.86	60.86	60.86
C_p° (cal/mol K)	9.45	9.90	9.89	9.93	9.93	9.93	9.93
Sarin							
ΔH_f° (kcal/mol)	--	-70.97	-67.4	-66.92	-68.34		
S° (cal/mol K)	--	100.07	99.54	99.86	99.86		
C_p° (cal/mol K)	--	34.87	34.66	34.65	34.65		

^a CCSD(T)/ ∞ (Q)Z: b2plypd3/6-311+(2d,d,p)//ccsd(t)[DZ+TZ]/mp2[DZ+TZ+QZ]

^b QCISD(T)/ ∞ (Q)Z: b2plypd3/6-311+(2d,d,p)//qcisd(t)[DZ+TZ]/mp2[DZ+TZ+QZ]

^c CCSD(T)/ ∞ QZ: b2plypd3/6-311+(2d,d,p)//ccsd(t)[TZ+QZ]

^d QCISD(T)/ ∞ QZ: b2plypd3/6-311+(2d,d,p)//qcisd(t)[TZ+QZ]

Table S2: Parameters used in the master equation simulation of the molecular decomposition of sarin and its simulants.

Species	$\langle E_{down} \rangle$ (cm ⁻¹)	σ (Å)	ϵ (K)
N2	250	3.621	97.53
Sarin		6.020	701.584
DIMP		6.940	603.276
DEMP		6.377	587.218
TEP		5.936	629.241

The collisional energy transfer probability was described by the exponential down model, with $\langle E_{down} \rangle = \langle E_{down} \rangle \times (T/300)^{0.85}$ (cm⁻¹). The Lennard-Jones parameter were calculated from the method proposed by Tee et al. (L.S. Tee, S. Gotoh, W.E. Stewart, Molecular Parameters for Normal Fluids. Lennard-Jones 12-6 Potential, Industrial & Engineering Chemistry Fundamentals. 5 (1966) 356–363).

Table S3: High-pressure limit (k_∞) and dependent pressure rate constants calculated for the molecular decomposition of sarin and its simulants calculated using the QCISD(T)/cc-PV ∞ QZ//B2PLYPD3/6-311+G(2d,d,p) level of theory.

Reaction channel	P (atm)	$k(T) = A T^n e^{-E/RT}$			T (K)
		A	n	E	
Sarin = POF[OH]me+C3H6 (TS1)	k_∞	7.017×10^8	1.191	3727	500- 2000
	0.01	2.130×10^{48}	-10.969	5285	500- 2000
	0.1	4.179×10^{39}	-8.173	5031	500- 2000
	1	8.578×10^{27}	-4.577	4572	500- 2000
	10	9.570×10^{16}	-1.270	4092	500- 2000
	100	3.442×10^{10}	0.657	3795	500- 2000
POF[OH]me = CH3PO2+HF (TS2)	k_∞	5.419×10^{10}	0.666	4948	500- 2000
	0.01	6.846×10^{45}	-10.109	6360	500- 2000
	0.1	4.678×10^{36}	-7.202	6061	500- 2000
	1	6.934×10^{25}	-3.880	5626	500- 2000
	10	6.421×10^{16}	-1.153	5229	500- 2000
	100	1.320×10^{12}	0.250	5013	500- 2000
TEP = DEP+C2H4 (TS3)	k_∞	2.278×10^6	1.841	3856	500- 2000
	0.01	1.184×10^{47}	-10.503	5570	500- 2000
	0.1	1.944×10^{35}	-6.846	5133	500-

				0	2000
	1	2.730×10^{22}	-2.946	4585 0	500- 2000
	10	2.726×10^{12}	0.053	4130 0	500- 2000
	100	6.540×10^7	1.430	3913 0	500- 2000
<hr/>					
DEP = MEP+C2H4 (TS4)	k_{∞}	1.097×10^5	2.214	3846 0	500- 2000
	0.01	4.717×10^{46}	-10.446	5598 0	500- 2000
	0.1	2.306×10^{35}	-6.913	5195 0	500- 2000
	1	3.181×10^{22}	-2.999	4657 0	500- 2000
	10	1.168×10^{12}	0.136	4187 0	500- 2000
	100	7.542×10^6	1.684	3944 0	500- 2000
<hr/>					
DEP = C2H5OPO2+C2H5OH (TS5)	k_{∞}	6.222×10^4	2.053	3646 0	500- 2000
	0.01	8.661×10^{43}	-9.791	5299 0	500- 2000
	0.1	1.308×10^{33}	-6.420	4906 0	500- 2000
	1	1.128×10^{21}	-2.752	4398 0	500- 2000
	10	2.491×10^{11}	0.147	3962 0	500- 2000
	100	4.547×10^6	1.560	3740 0	500- 2000
<hr/>					
MEP = PO[OH]3+C2H4 (TS6)	k_{∞}	1.747×10^5	2.048	3829 0	500- 2000
	0.01	5.494×10^{45}	-10.329	5472 0	500- 2000
	0.1	2.219×10^{36}	-7.333	5183	500-

				0	2000
	1	2.289×10^{24}	-3.653	4706 0	500- 2000
	10	4.176×10^{13}	-0.412	4234 0	500- 2000
	100	3.788×10^7	1.394	3955 0	500- 2000
<hr/>					
MEP = HOPO2+C2H5OH (TS7)	k_{∞}	1.216×10^5	2.013	3611 0	500- 2000
	0.01	1.406×10^{43}	-9.603	5159 0	500- 2000
	0.1	8.660×10^{33}	-6.685	4861 0	500- 2000
	1	4.302×10^{22}	-3.222	4404 0	500- 2000
	10	5.452×10^{12}	-0.239	3967 0	500- 2000
	100	1.887×10^7	1.393	3714 0	500- 2000
<hr/>					
C2H5OPO2 = HOPO2+C2H4 (TS8)	k_{∞}	4.192×10^7	1.542	3600 0	500- 2000
	0.01	1.457×10^{44}	-9.863	4974 0	500- 2000
	0.1	8.426×10^{37}	-7.769	4854 0	500- 2000
	1	9.081×10^{27}	-4.654	4498 0	500- 2000
	10	2.801×10^{17}	-1.457	4055 0	500- 2000
	100	3.035×10^{10}	0.634	3740 0	500- 2000
<hr/>					
MEP = C2H5OPO2+H2O (TS9)	k_{∞}	9.220×10^4	2.093	3917 0	500- 2000
	0.01	1.117×10^{46}	-10.520	5562 0	500- 2000
	0.1	4.358×10^{36}	-7.510	5278	500-

				0	2000
	1	2.998×10^{24}	-3.772	4796 0	500- 2000
	10	3.308×10^{13}	-0.464	4315 0	500- 2000
	100	2.168×10^7	1.385	4029 0	500- 2000
<hr/>					
TEP = C2H5OPO2+C2H5OH+C2H4	k_{∞}	4.394×10^3	2.521	5174 0	500- 2000
(TS10)	0.01	1.560×10^{60}	-14.774	7493 0	500- 2000
	0.1	2.926×10^{45}	-10.133	6999 0	500- 2000
	1	4.880×10^{27}	-4.710	6264 0	500- 2000
	10	8.917×10^{12}	-0.281	5602 0	500- 2000
	100	7.001×10^5	1.839	5269 0	500- 2000
<hr/>					
PO[OH]3 = HOPO2+H2O (TS11)	k_{∞}	9.093×10^4	2.115	3891 0	500- 2000
	0.01	9.440×10^{36}	-7.810	5155 0	500- 2000
	0.1	8.311×10^{28}	-5.224	4914 0	500- 2000
	1	8.081×10^{18}	-2.139	4522 0	500- 2000
	10	3.102×10^{10}	0.405	4155 0	500- 2000
	100	1.989×10^6	1.661	3963 0	500- 2000
<hr/>					
DIMP = IMP+C3H6 (TS12)	k_{∞}	8.796×10^7	1.495	3858 9	500- 2000
	0.01	2.205×10^{50}	-11.428	5622 6	500- 2000
	0.1	2.705×10^{39}	-8.010	5242	500-

				3	2000
	1	3.557×10^{26}	-4.084	4707 2	500- 2000
	10	3.562×10^{15}	-0.780	4212 0	500- 2000
	100	1.536×10^{10}	0.820	3960 4	500- 2000
<hr/>					
IMP = MPA+C3H6 (TS13)	k_{∞}	3.845×10^8	1.184	3840 6	500- 2000
	0.01	2.211×10^{45}	-9.974	5384 0	500- 2000
	0.1	1.720×10^{34}	-6.516	4978 9	500- 2000
	1	1.390×10^{22}	-2.843	4466 5	500- 2000
	10	1.403×10^{13}	-0.144	4058 3	500- 2000
	100	2.172×10^9	0.992	3879 5	500- 2000
<hr/>					
IMP = CH3PO2+iC3H7OH (TS14)	k_{∞}	2.840×10^9	0.760	3608 2	500- 2000
	0.01	3.123×10^{43}	-9.608	5014 3	500- 2000
	0.1	2.430×10^{33}	-6.437	4663 8	500- 2000
	1	7.938×10^{21}	-2.940	4184 0	500- 2000
	10	2.541×10^{13}	-0.389	3800 6	500- 2000
	100	1.056×10^{10}	0.620	3642 4	500- 2000
<hr/>					
DIMP = CH3PO2+C3H6Y+iC3H7OH (TS15)	k_{∞}	9.784×10^6	1.547	5363 0	500- 2000
	0.01	3.010×10^{65}	-16.353	7715 2	500- 2000
	0.1	1.760×10^{52}	-12.121	7318	500-

				2	2000
	1	4.482×10^{-34}	-6.724	6614 8	500- 2000
	10	4.408×10^{-18}	-1.902	5905 0	500- 2000
	100	1.243×10^{10}	0.651	5506 9	500- 2000
<hr/>					
MPA = CH ₃ PO ₂ +H ₂ O (TS16)	k_{∞}	5.329×10^9	0.979	3981 4	500- 2000
	0.01	9.477×10^{43}	-9.778	5314 5	500- 2000
	0.1	2.255×10^{36}	-7.299	5110 5	500- 2000
	1	7.771×10^{25}	-4.062	4711 2	500- 2000
	10	1.721×10^{16}	-1.139	4294 1	500- 2000
	100	7.309×10^{10}	0.470	4048 5	500- 2000
<hr/>					
DEMP = EMP+C ₂ H ₄ (TS17)	k_{∞}	1.208×10^5	2.218	3949 7	500- 2000
	0.01	6.266×10^{41}	-8.855	5546 3	500- 2000
	0.1	9.484×10^{28}	-4.925	5032 0	500- 2000
	1	6.352×10^{16}	-1.253	4495 7	500- 2000
	10	8.358×10^8	1.103	4131 2	500- 2000
	100	1.278×10^6	1.941	3997 7	500- 2000
<hr/>					
EMP = MPA+C ₂ H ₄ (TS18)	k_{∞}	3.287×10^6	1.653	3972 3	500- 2000
	0.01	3.192×10^{40}	-8.645	5437 3	500- 2000
	0.1	3.195×10^{28}	-4.952	4966	500-

				9	2000
	1	9.657×10^{16}	-1.471	4464 3	500- 2000
	10	4.279×10^9	0.729	4126 1	500- 2000
	100	1.177×10^7	1.492	4005 3	500- 2000
<hr/>					
EMP = CH ₃ PO ₂ +C ₂ H ₅ OH (TS19)	k_{∞}	3.710×10^9	0.728	3635 5	500- 2000
	0.01	1.435×10^{43}	-9.533	5008 7	500- 2000
	0.1	3.183×10^{33}	-6.489	4684 8	500- 2000
	1	1.661×10^{22}	-3.047	4218 9	500- 2000
	10	4.629×10^{13}	-0.475	3834 9	500- 2000
	100	1.407×10^{10}	0.575	3670 9	500- 2000
<hr/>					
DEMP = CH ₃ PO ₂ +C ₂ H ₅ OH+C ₂ H ₄ Z (TS20)	k_{∞}	2.764×10^4	2.342	5510 0	500- 2000
	0.01	1.838×10^{26}	-4.124	6520 0	500- 2000
	0.1	3.025×10^{14}	-0.595	5981 0	500- 2000
	1	4.558×10^7	1.437	5659 0	500- 2000
	10	2.090×10^5	2.132	5547 0	500- 2000
	100	8.155×10^4	2.253	5527 0	500- 2000

Units are mole, s, cal, and K. Rates computed with nitrogen as the bath gas.

Table S4: Optimized geometries (Cartesian coordinates), electronic energies at 0 K and ZPE (in hartree) at the QCISD(T)/cc-PV ∞ QZ//B2PLYPD3/6-311+G(2d,d,p) level of theory of the species and transition states (TS) from Table S1.

Sarin			
$E_{0K} = -749.3093160$ $ZPE = 0.1454320$			
P	1.044142	-0.003323	0.165717
O	1.133422	0.162143	1.618440
F	1.338853	1.364267	-0.606280
C	2.180513	-1.116003	-0.640718
H	2.055410	-2.112573	-0.217973
H	3.197789	-0.769619	-0.457560
H	1.982747	-1.140188	-1.711978
O	-0.362777	-0.433592	-0.419798
C	-1.615286	-0.063929	0.254273
C	-2.076744	1.286743	-0.264522
C	-2.590045	-1.189320	-0.029248
H	-1.397545	-0.007341	1.322793
H	-1.342539	2.064005	-0.048263
H	-3.018854	1.562004	0.215601
H	-2.233936	1.244079	-1.344456
H	-2.202008	-2.137742	0.344456
H	-2.765454	-1.279205	-1.103457
H	-3.543208	-0.985326	0.463754

TEP			
$E_{0K} = -878.9044208$ $ZPE = 0.2206430$			
O	-0.000367	-0.009280	1.782593
P	0.002466	-0.002686	0.312269
O	-0.200356	1.412970	-0.373901
O	1.329565	-0.528879	-0.379380
O	-1.118297	-0.882412	-0.384948
C	-1.248274	2.291822	0.110908
C	-1.019893	3.657689	-0.497369
C	2.614844	-0.067423	0.111290
C	3.682667	-0.947033	-0.500006
C	-1.362627	-2.230253	0.093834
C	-2.679216	-2.693628	-0.488927
H	-2.210157	1.873200	-0.194690
H	-1.203011	2.319387	1.201216
H	-1.804836	4.343214	-0.168878
H	-0.054914	4.059681	-0.184675
H	-1.039748	3.601230	-1.586733
H	2.736546	0.976513	-0.187463
H	2.613376	-0.127351	1.201231
H	4.668844	-0.615029	-0.166507
H	3.544534	-1.985407	-0.194605
H	3.646927	-0.894264	-1.589150
H	-0.534310	-2.861741	-0.236221
H	-1.384413	-2.213889	1.185080
H	-2.885270	-3.716918	-0.165820
H	-3.494542	-2.052111	-0.150889
H	-2.645377	-2.672465	-1.579217

POF[OH]me			
$E_{0K} = -631.6164489$ $ZPE = 0.0601410$			
P	0.088638	-0.087266	-0.097978
O	0.629343	1.414551	-0.017473
F	0.188584	-0.548983	1.419159
C	-1.668685	0.125606	-0.293768
H	-1.867086	0.494753	-1.299618
H	-2.043480	0.835417	0.443193
H	-2.154425	-0.840776	-0.159272
O	0.808145	-0.974304	-1.011096
H	1.550357	1.484829	-0.295899

H	-3.130743	0.602280	-1.122751
O	1.107512	-1.087995	-1.035626
H	1.845055	-1.663226	-0.804009
O	1.660489	1.258343	-0.419791
H	1.855218	1.871656	0.297296

DEP			
$E_{0K} = -800.4516790$ $ZPE = 0.1634360$			
O	-0.027999	1.196630	1.476432
P	0.014015	0.725364	0.085571
O	1.389700	0.117014	-0.426990
O	-1.014196	-0.419030	-0.298322
C	2.012496	-0.942291	0.339945
C	3.405190	-1.148500	-0.215030
C	-2.399664	-0.301273	0.119633
C	-3.068284	-1.634777	-0.128778
H	2.033326	-0.646326	1.390718
H	1.405863	-1.844516	0.234488
H	3.906489	-1.944108	0.329127
H	3.362650	-1.407749	-1.271712
H	3.993384	-0.227676	-0.107510
H	-2.421953	-0.025059	1.175390
H	-2.863976	0.494979	-0.466920
H	-4.120974	-1.577556	0.158185
H	-3.894600	-1.903503	-1.184420
H	-2.590248	-2.418740	0.460583
O	-0.281490	1.855553	-1.479600
H	-0.055570	2.729014	-0.666704

MEP			
$E_{0K} = -721.9986204$ $ZPE = 0.1061960$			
P	0.830748	0.001202	0.099044
O	1.129330	-0.432102	1.469013
O	-0.653969	0.435589	-0.219190
C	-1.745642	-0.454987	0.142127
H	-1.620689	-0.750069	1.185633
H	-1.681726	-1.342565	-0.491114
C	-3.039245	0.295180	-0.080101
H	-3.884455	-0.350686	0.169197
H	-3.081460	1.182743	0.552693

DEMP			
$E_{0K} = -764.4845429$ $ZPE = 0.1863820$			
O	0.501988	0.638930	1.598191
P	0.147645	0.811111	0.176558
O	1.113448	-0.005946	-0.816312
O	-1.312643	0.329147	-0.256762
C	2.314409	-0.653359	-0.326003
C	2.035209	-2.097277	0.040666
C	-1.764639	-0.992966	0.123002
C	-3.242428	-1.084826	-0.188399
H	3.028470	-0.581304	-1.146675
H	2.695439	-0.100930	0.533905
H	2.965646	-2.591642	0.332802
H	1.341772	-2.148994	0.881328
H	1.611135	-2.635145	-0.809637
H	-1.191316	-1.728874	-0.446776
H	-1.567805	-1.137457	1.187518
H	-3.614114	-2.078201	0.074531
H	-3.800764	-0.342187	0.383434
H	-3.421973	-0.916021	-1.251307
C	0.139298	2.483449	-0.457853
H	-0.105106	2.480190	-1.519805
H	-0.598191	3.069951	0.090235
H	1.128689	2.916784	-0.307336

EMP			
$E_{0K} = -686.0327748$ $ZPE = 0.1292510$			
P	0.823533	-0.062572	0.121477
C	1.754915	1.451492	-0.057122
H	2.817696	1.215720	0.001206
H	1.531306	1.916991	-1.016709
H	1.489312	2.129930	0.753511

O	1.062438	-0.874612	1.328147
O	-0.660037	0.473959	-0.105275
C	-1.776459	-0.447018	-0.007196
H	-1.671210	-1.025665	0.912641
H	-1.733941	-1.126326	-0.862059
C	-3.049928	0.369295	-0.011640
H	-3.914267	-0.296527	0.047526
H	-3.073568	1.046118	0.843620
H	-3.126271	0.957745	-0.927193
O	1.128270	-0.895450	-1.235189
H	1.511423	-1.753189	-1.020410

DIMP			
$E_{0K} = -842.9646850$ $ZPE = 0.2421750$			
C	-2.234890	-0.511892	0.187036
O	-1.056174	-0.034703	-0.529266
C	-3.332500	-0.660852	-0.850408
C	-1.892104	-1.811785	0.894201
C	1.964612	-0.778981	-0.121558
O	1.374109	0.506719	-0.485795
C	2.594431	-1.334353	-1.384565
C	2.951045	-0.561689	1.012831
C	-0.241242	2.552312	-0.606116
P	-0.004388	0.958090	0.174270
O	-0.087535	0.939716	1.647803
H	-2.510421	0.242056	0.928667
H	-4.252578	-1.009703	-0.375380
H	-3.533516	0.293431	-1.340001
H	-3.036486	-1.386028	-1.611682
H	-2.773523	-2.203136	1.408767
H	-1.107967	-1.643794	1.633078
H	-1.555166	-2.556740	0.168605
H	1.157621	-1.440517	0.206924
H	3.052773	-2.304929	-1.179552
H	1.841882	-1.458984	-2.164402
H	3.367660	-0.654368	-1.749254
H	3.401639	-1.514452	1.303210
H	2.445208	-0.132099	1.877798
H	3.746047	0.116110	0.693140
H	0.525787	3.241037	-0.251174
H	-1.222839	2.935555	-0.323615

H	-0.179614	2.454796	-1.689628
---	-----------	----------	-----------

CH3PO2			
$E_{0K} = -531.1534213$ $ZPE = 0.0454020$			
P	0.196169	-0.000021	-0.005943
O	0.786778	1.341150	0.003736
O	0.786110	-1.341486	0.003736
C	-1.607931	0.000346	-0.004478
H	-1.971465	0.903999	-0.489385
H	-1.971724	-0.901548	-0.492485
H	-1.934850	-0.001524	1.038103

HF			
$E_{0K} = -100.3898240$ $ZPE = 0.0094360$			
F	-0.050656	-0.123140	-0.001618
H	-0.969781	-0.123140	-0.001618

IMP			
$E_{0K} = -725.2726867$ $ZPE = 0.1572700$			
P	1.047497	-0.113929	0.054007
O	1.198423	-1.482645	0.582161
C	2.130727	0.375043	-1.281160
H	1.926485	-0.249282	-2.150982
H	3.163576	0.227426	-0.964679
H	1.966838	1.422676	-1.532257
O	-0.368066	0.288013	-0.548741
C	-1.591395	0.029748	0.211960
C	-2.516423	1.200642	-0.057901
C	-2.156784	-1.313011	-0.215842
H	-1.329615	0.003252	1.273724
H	-2.052582	2.136360	0.256771
H	-3.453003	1.071222	0.489728
H	-2.742660	1.262374	-1.124683
H	-1.436437	-2.107936	-0.021751
H	-2.392183	-1.297203	-1.282557
H	-3.073889	-1.524881	0.339827
O	1.281093	0.998494	1.211028
H	1.622665	0.579497	2.008821

MPA			
$E_{0K} = -607.5800937$ $ZPE = 0.0716710$			
P	0.083251	0.000264	0.111708
C	-1.696547	-0.076731	0.205760

H	-2.058579	0.778499	0.775608
H	-2.120975	-0.056124	-0.798215
H	-1.982691	-1.001513	0.705972
O	0.874018	-0.026747	1.354494
O	0.424445	-1.220323	-0.884135
H	1.227849	-1.677198	-0.610396
O	0.292802	1.329113	-0.771165
H	1.134802	1.756425	-0.576698

Ethene			
$E_{0K} = -78.4316911$ $ZPE = 0.0510780$			
C	-0.666357	0.000000	-0.000003
C	0.666357	0.000000	0.000003
H	-1.234556	0.922928	0.000010
H	-1.234556	-0.922928	-0.000022
H	1.234556	-0.922928	-0.000010
H	1.234556	0.922928	0.000023

Propene			
$E_{0K} = -117.6687885$ $ZPE = 0.0798700$			
C	1.280568	-0.221993	-0.000007
C	0.132333	0.458228	-0.000009
H	2.238903	0.282757	-0.000025
H	1.294232	-1.307132	0.000013
H	0.166947	1.545389	-0.000031
C	-1.232820	-0.163682	0.000013
H	-1.804622	0.148756	-0.879223
H	-1.171337	-1.253876	0.000033
H	-1.804607	0.148788	0.879247

C2H5OPO2			
$E_{0K} = -645.5683202$ $ZPE = 0.0801830$			
P	-0.964129	0.063243	0.002649
O	-0.735964	1.504023	0.138965
O	-2.135032	-0.731401	-0.351253
O	0.302430	-0.822824	0.297523
C	1.603717	-0.218666	0.614649
H	1.433840	0.672967	1.216149
H	2.097467	-0.981129	1.213862
C	2.362262	0.091630	-0.656034
H	3.356555	0.465910	-0.400348
H	2.476417	-0.804496	-1.267493

H	1.850297	0.861937	-1.235473
isopropanol			
$E_{0K} = -194.0461381$ $ZPE = 0.1086370$			
C	-1.189196	-0.788012	-0.103393
C	0.002684	0.037982	0.366677
C	1.329264	-0.542301	-0.091086
O	-0.056321	1.370385	-0.160522
H	-1.199068	-0.845737	-1.194452
H	-1.142015	-1.802185	0.301633
H	-2.132040	-0.341340	0.226337
H	-0.005854	0.086497	1.464242
H	1.468051	-1.547485	0.313365
H	1.357425	-0.595774	-1.182010
H	2.154618	0.087091	0.245059
H	-0.907057	1.749837	0.076812

C2H5OH			
$E_{0K} = -154.8068060$ $ZPE = 0.0803530$			
C	-1.220747	-0.223745	0.000049
C	0.081765	0.550251	0.000094
O	1.151593	-0.396544	-0.000132
H	-2.070915	0.462424	0.000275
H	-1.284919	-0.858747	0.885348
H	-1.285087	-0.858380	-0.885499
H	0.139120	1.192924	-0.886914
H	0.139236	1.192624	0.887313
H	1.983715	0.082477	-0.000334

PO[OH]3			
$E_{0K} = -643.5452212$ $ZPE = 0.0489970$			
P	0.078822	0.048227	0.110991
O	1.050219	0.427952	1.131426
O	-0.984483	1.178295	-0.217769
H	-1.641689	0.920114	-0.873877
O	0.728208	-0.375488	-1.296671
H	1.582644	0.050940	-1.428741
O	-0.883573	-1.193254	0.384409
H	-0.406259	-1.994505	0.626593

HOPO2			
$E_{0K} = -567.1130075$ $ZPE = 0.0230520$			
P	-0.087552	0.111934	-0.000256
O	0.791468	1.280669	0.000135
O	-1.530504	-0.080306	0.000248
O	0.696372	-1.268213	-0.000076
H	1.654588	-1.136204	0.001373

H2O			
$E_{0K} = -76.3604671$ $ZPE = 0.0214820$			
O	0.000000	0.000000	0.117425
H	0.000000	0.759443	-0.469701
H	0.000000	-0.759443	-0.469701

TS1-1			
$E_{0K} = -749.2479917$ $ZPE = 0.1384340$			
P	-1.000933	-0.016602	-0.029531
O	-0.547715	1.180542	-0.840094
F	-1.600396	-1.086549	-1.056603
C	-2.458113	0.346622	0.943009
H	-2.201484	1.090791	1.697307
H	-3.240485	0.742271	0.294418
H	-2.807684	-0.562931	1.432581
O	0.082482	-0.688156	0.770584
C	2.101847	0.127073	0.536942
C	2.014569	1.331246	-0.185682
C	2.613617	-1.128844	-0.062593
H	2.010794	0.150966	1.615031
H	0.813499	1.322495	-0.532990
H	2.097971	2.247532	0.393088
H	2.520661	1.340704	-1.149482
H	2.213290	-2.005085	0.440735
H	2.395553	-1.175789	-1.130196
H	3.705793	-1.118650	0.057925

TS1-2			
$E_{0K} = -749.2476337$ $ZPE = 0.138397$			
P	1.010832	-0.016587	0.017227
O	0.577628	-1.212645	-0.805729
O	-0.106163	0.711162	0.716110
C	-2.120262	-0.097450	0.437059
C	-2.032924	-1.250571	-0.364245
C	-2.633016	1.198200	-0.070473
H	-2.035340	-0.199276	1.511181
H	-0.809520	-1.286540	-0.622150
H	-2.166027	-2.199110	0.150988
H	-2.497160	-1.184178	-1.346223
H	-2.233909	2.036730	0.494470
H	-2.418460	1.321119	-1.132822
H	-3.724937	1.177853	0.050404
C	2.077265	1.079534	-0.911736
H	1.504564	1.520962	-1.727686
H	2.449375	1.869494	-0.258481
H	2.914542	0.513164	-1.321153
F	2.037366	-0.543091	1.124044

TS2			
$E_{0K} = -631.5350160$ $ZPE = 0.0548630$			
P	0.224885	-0.237317	0.125515
O	-0.853949	-0.184814	1.196606
F	-1.414569	0.434885	-0.877780
C	1.182309	1.268290	0.009583
H	1.640392	1.323186	-0.976488
H	1.966510	1.213538	0.768362
H	0.545789	2.129433	0.200132
O	0.816635	-1.421733	-0.480036
H	-1.590189	0.222261	0.235234

TS3			
$E_{0K} = -878.8389944$ $ZPE = 0.213689$			
P	0.119001	-0.075085	-0.13227900
O	0.653077	-0.276463	1.28400400
O	1.201426	-0.131306	-1.18149500
C	2.982578	-0.948007	-0.63013600
C	3.071317	-1.116483	0.76005000

H	2.743314	-1.779582	-1.27741300
H	1.890697	-0.708725	1.12556000
H	3.061074	-2.139291	1.12720900
H	3.727733	-0.434860	1.29393200
H	3.431025	-0.095748	-1.11933600
O	-0.713212	1.281539	-0.19766800
C	-0.057637	2.525525	0.14273500
H	0.769257	2.682149	-0.55447400
H	0.342888	2.441007	1.15564100
C	-1.084026	3.632374	0.03968400
H	-0.620915	4.590890	0.28655400
H	-1.484959	3.689616	-0.97336700
H	-1.908023	3.456363	0.73307300
O	-1.003266	-1.135618	-0.48644400
C	-2.157672	-1.284991	0.37690300
H	-1.812685	-1.379262	1.40910300
H	-2.767858	-0.383752	0.28830300
C	-2.912465	-2.516281	-0.07379400
H	-2.286967	-3.405472	0.01878700
H	-3.802916	-2.650280	0.54541900
H	-3.223443	-2.414809	-1.11462600

TS4

$E_{0K} = -800.3857423$ ZPE = 0.156340

P	-0.091679	0.628363	0.02952600
O	-0.694847	0.248759	1.36742400
O	-0.755576	-0.064078	-1.14287400
C	-2.543731	-0.990200	-0.78277100
C	-2.825913	-1.051107	0.58970700
H	-2.997529	-0.237861	-1.41163800
H	-1.800803	-0.422183	1.07202200
H	-3.640597	-0.427172	0.94728200
H	-2.739323	-2.025167	1.06329100
H	-2.118100	-1.834831	-1.30448300
O	1.481081	0.384569	-0.00855200
C	1.976247	-0.975612	0.04279100
H	1.561848	-1.526923	-0.80441700
H	1.627653	-1.434197	0.97149300
C	3.486979	-0.919944	-0.01282600

H	3.895747	-1.932495	0.02848500
H	3.819236	-0.448686	-0.93913200
H	3.880252	-0.350680	0.83052500
O	-0.147609	2.217979	-0.09263900
H	0.260915	2.538092	-0.90459100

TS5

$E_{0K} = -800.3873121$ ZPE = 0.159687

P	0.037475	-0.942205	0.140733
O	-0.892428	-1.549797	1.087703
O	-0.777169	0.368918	-0.811648
C	-2.201072	0.636470	-0.623422
H	-2.725080	-0.318125	-0.556503
H	-2.514089	1.166561	-1.522530
C	-2.391809	1.466705	0.626832
H	-3.452816	1.694762	0.752937
H	-2.054369	0.914674	1.504672
H	-1.840362	2.405586	0.555096
O	0.424225	-1.462481	-1.249294
H	-0.349561	-0.439691	-1.574949
O	1.244087	-0.225196	0.853427
C	2.391421	0.312362	0.133587
H	2.511777	-0.242885	-0.796687
H	3.239823	0.106637	0.784715
C	2.216660	1.798394	-0.104260
H	3.112215	2.196439	-0.588221
H	1.358243	1.990708	-0.748718
H	2.071175	2.323272	0.841262

TS6

$E_{0K} = -721.9324434$ ZPE = 0.099221

P	-0.705534	-0.006932	0.016718
O	-0.030337	1.355540	-0.070601
O	0.237187	-1.121766	0.375481
C	2.244968	-0.740899	0.098704
C	2.485713	0.624700	-0.107718
H	2.368470	-1.191861	1.072279
H	1.278378	1.084340	-0.094748
H	2.949331	1.168041	0.711010
H	2.805664	0.916188	-1.104621
H	2.198805	-1.431696	-0.730932
O	-1.962692	0.094433	1.004787
H	-1.732382	0.513857	1.840841

O	-1.443864	-0.395059	-1.342218
H	-2.071687	0.277121	-1.630100

TS7

$E_{0K} = -721.9341888$ $ZPE = 0.102522$

P	-0.859730	0.178082	-0.1517390
O	-0.532833	1.597766	-0.210587
O	0.504681	-0.774569	0.510563
C	1.785930	-0.142508	0.827840
H	2.298049	-0.851946	1.476273
H	1.542899	0.758277	1.390506
C	2.580629	0.174621	-0.421721
H	3.539970	0.611406	-0.134596
H	2.780374	-0.730848	-0.999142
H	2.049138	0.892228	-1.047019
O	-0.828163	-0.862414	-1.275672
H	0.223350	-1.239510	-0.548359
O	-2.060512	-0.121475	0.845138
H	-2.402570	-1.017969	0.746174

TS8

$E_{0K} = -645.5090966$ $ZPE = 0.073045$

O	-0.256183	1.332140	-0.000001
O	-0.033792	-1.167361	0.000011
C	2.042901	-0.764086	-0.000011
C	2.279996	0.614695	0.000004
H	2.055993	-1.338725	0.915226
H	1.083703	1.042112	0.000001
H	2.666050	1.045027	0.920127
H	2.666061	1.045043	-0.920106
H	2.055971	-1.338694	-0.915268
P	-0.978468	0.001882	0.000003
O	-2.433543	-0.113110	-0.000007

TS9

$E_{0K} = -721.9457965$ $ZPE = 0.105679$

P	-0.821515	0.300462	0.134389
O	-1.665642	1.450835	-0.160522
O	-1.289520	-1.152927	-0.934950
O	-0.998522	-0.726285	1.253914
H	-1.372059	-1.452870	0.209285
O	0.689583	0.524055	-0.227543
C	1.712491	-0.485680	0.028105
H	1.595930	-1.267598	-0.724667

H	1.539142	-0.909741	1.017054
C	3.056050	0.198573	-0.073486
H	3.849372	-0.533743	0.094170
H	3.191586	0.639293	-1.061783
H	3.144319	0.984874	0.677160
H	-2.123991	-1.009926	-1.401966

TS10

$E_{0K} = -878.8161202$ $ZPE = 0.213530$

O	-0.945837	0.591383	1.785352
P	-0.007546	-0.174352	0.953621
O	0.254488	0.754218	-0.499255
O	1.396672	-0.539687	1.338933
O	-0.631980	-1.464295	0.245181
C	0.465765	2.191859	-0.337321
C	-0.845102	2.926617	-0.515865
C	2.600245	-1.220361	-0.301487
C	2.313774	-0.524637	-1.470722
C	-2.044330	-1.525148	-0.074150
C	-2.283088	-1.165524	-1.528752
H	0.900999	2.371505	0.646649
H	1.194036	2.465870	-1.103285
H	-0.673639	4.002964	-0.430264
H	-1.269824	2.720696	-1.500158
H	-1.550370	2.620401	0.255779
H	3.400003	-0.917158	0.357687
H	2.169202	-2.192915	-0.111643
H	3.009394	0.248923	-1.783453
H	1.806461	-1.065088	-2.265091
H	1.266273	0.181628	-1.016840
H	-2.339428	-2.554232	0.131930
H	-2.585688	-0.861214	0.601257
H	-3.344378	-1.277381	-1.766384
H	-1.988828	-0.134359	-1.726583
H	-1.711341	-1.824154	-2.185833

TS11

$E_{0K} = -643.4766710$ $ZPE = 0.045369$

P	0.186656	0.077400	0.163260
O	0.862392	1.373114	0.147263
O	-1.284709	0.092866	-0.944039
O	-0.796747	-0.484668	1.173654
H	-1.609396	-0.273753	0.137377

H	-1.558171	0.991258	-1.176079
O	1.038342	-1.116340	-0.438450
H	1.813511	-0.798294	-0.917619

TS12

$E_{0K} = -842.9013586$ $ZPE = 0.2353400$

P	0.005034	0.770218	0.000975
O	0.338573	0.594303	1.484480
O	0.805466	-0.182011	-0.874669
C	2.469786	-1.151162	-0.017863
C	2.431488	-0.980433	1.379371
C	3.454001	-0.439750	-0.878562
H	1.996123	-2.022710	-0.449944
H	1.424879	-0.206013	1.516157
H	2.125562	-1.846818	1.960720
H	3.243817	-0.398269	1.810357
H	3.103017	-0.355101	-1.904238
H	3.680639	0.550621	-0.480045
H	4.383777	-1.023491	-0.868290
O	-1.567394	0.588597	-0.235422
C	0.204327	2.477060	-0.509855
H	1.254071	2.753128	-0.400112
H	-0.093166	2.586632	-1.553179
H	-0.408108	3.124636	0.118173
C	-2.191804	-0.687798	0.082153
H	-1.514329	-1.246471	0.735349
C	-3.473113	-0.377306	0.833712
H	-3.990210	-1.303414	1.097481
H	-3.252131	0.174446	1.748323
H	-4.136432	0.227182	0.210649
C	-2.411518	-1.450546	-1.213590
H	-1.460393	-1.608378	-1.723073
H	-2.870394	-2.421239	-1.006982
H	-3.074389	-0.885521	-1.873291

TS13

$E_{0K} = -725.2084308$ $ZPE = 0.1501250$

P	-1.010516	-0.032462	-0.032608
O	-0.583117	-1.228404	0.817112
O	0.110213	0.470868	-0.923223
C	2.088901	-0.154372	-0.450860

C	2.021328	-1.220233	0.466170
C	2.527769	1.210732	-0.055535
H	2.100702	-0.375411	-1.509836
H	0.772721	-1.284373	0.693617
H	2.223196	-2.210755	0.065797
H	2.437992	-1.026249	1.452698
H	2.137843	1.968746	-0.730458
H	2.233679	1.437289	0.970635
H	3.624814	1.227707	-0.098613
O	-2.314878	-0.413433	-0.901827
H	-2.151188	-1.160037	-1.488782
C	-1.704844	1.274088	0.979506
H	-0.926910	1.650930	1.644523
H	-2.061842	2.084367	0.343145
H	-2.529920	0.881176	1.574217

TS14

$E_{0K} = -725.2106489$ $ZPE = 0.1530060$

P	-1.220582	-0.071621	-0.209717
O	-1.157283	0.796031	-1.392151
O	0.438463	-0.425466	0.463580
C	1.643451	0.034339	-0.241138
H	1.447935	-0.067082	-1.311469
C	1.853130	1.493689	0.112490
H	2.739723	1.872710	-0.400744
H	0.997365	2.090499	-0.205215
H	1.997946	1.606805	1.189332
O	-1.342602	-1.603239	-0.215027
H	-0.091834	-1.459126	0.198343
C	2.778571	-0.874785	0.187538
H	2.566981	-1.914294	-0.070349
H	3.698570	-0.578055	-0.320873
H	2.937531	-0.804495	1.265605
C	-2.065771	0.648601	1.197792
H	-3.137435	0.623926	0.989807
H	-1.859276	0.069043	2.096097
H	-1.753687	1.684709	1.323903

TS15

$E_{0K} = -842.8785159$ $ZPE = 0.2344580$

O	-1.170983	1.006612	-1.498108
P	-0.325901	1.128206	-0.292011

O	-0.472017	-0.341174	0.626628
O	1.176494	1.261116	-0.332261
C	-1.413304	-1.428560	0.357100
C	-2.840695	-0.922151	0.482815
C	2.637479	-0.193047	0.506716
C	1.941512	-1.133793	1.266568
H	-1.208055	-2.132911	1.169292
H	-3.531403	-1.765321	0.401674
H	-2.993920	-0.445557	1.452920
H	-3.060359	-0.208459	-0.311391
H	2.955356	0.729972	0.972969
H	1.953202	-2.161504	0.909280
H	1.940563	-1.005905	2.345429
H	0.740210	-0.750977	0.946503
C	-1.004602	2.299569	0.899910
H	-0.474968	2.228512	1.850394
H	-0.875486	3.304846	0.493839
H	-2.068492	2.112650	1.048115
C	-1.116282	-2.088800	-0.981333
H	-1.290379	-1.385777	-1.795010
H	-0.078750	-2.428923	-1.022718
H	-1.763656	-2.960786	-1.107171
C	3.185923	-0.489221	-0.839747
H	3.233698	0.406649	-1.452761
H	4.202799	-0.879703	-0.695644
H	2.600008	-1.256319	-1.347804

TS16

$E_{0K} = -607.5120713$ ZPE = 0.0678740

P	0.125944	0.210343	0.139516
O	0.332550	1.619457	-0.202815
O	-1.222037	-0.554545	-0.920207
O	-0.748676	-0.334634	1.272486
H	-1.501143	-0.657760	0.227452
H	-1.721876	0.109707	-1.415017
C	1.509122	-0.869985	-0.214800
H	1.945631	-0.604221	-1.176397
H	2.252959	-0.715792	0.569703
H	1.185835	-1.909386	-0.205391

TS17

$E_{0K} = -764.4184175$ ZPE = 0.1793750

P	-0.092173	0.615529	0.021116
O	-0.634740	0.121843	1.366296
C	-0.131034	2.402188	-0.082522
H	-1.169977	2.731610	-0.037468
H	0.422310	2.831028	0.753430
H	0.313178	2.725290	-1.024391
O	-0.813023	-0.039557	-1.150350
C	-2.548439	-1.003115	-0.777273
C	-2.797502	-1.122737	0.599267
H	-3.042686	-0.246239	-1.369333
H	-1.743552	-0.518650	1.082899
H	-3.608125	-0.522460	1.003233
H	-2.694736	-2.115846	1.028175
H	-2.131832	-1.825639	-1.340051
O	1.482638	0.357509	-0.066145
C	1.978779	-0.999817	0.009530
H	1.582678	-1.560730	-0.840380
H	1.613390	-1.452622	0.934377
C	3.490693	-0.942905	-0.019853
H	3.900578	-1.954646	0.031922
H	3.838666	-0.473319	-0.941235
H	3.868724	-0.370756	0.828775

TS18

$E_{0K} = -685.9652268$ ZPE = 0.1220960

P	0.696598	-0.062557	0.003526
O	-0.023023	-0.495754	1.282153
C	1.660056	1.423500	0.263092
H	0.980436	2.240097	0.509454
H	2.357110	1.271083	1.087538
H	2.210093	1.669783	-0.645528
O	-0.263673	0.074378	-1.167936
C	-2.245728	0.228971	-0.738546
C	-2.509534	-0.044529	0.612501
H	-2.194457	1.244681	-1.103780
H	-1.306184	-0.292461	1.043162
H	-2.805417	0.797247	1.232585
H	-3.012644	-0.982957	0.829454
H	-2.390299	-0.525435	-1.497800
O	1.878376	-1.096168	-0.344389
H	1.550189	-1.990984	-0.488889

TS19

$E_{0K} = -685.9700173$ ZPE = 0.1250920

P	0.880261	0.000226	0.229481
C	1.562210	1.219182	-0.893802
H	2.589511	1.418820	-0.582136
H	1.563395	0.831553	-1.911247
H	0.987092	2.142113	-0.829875
O	0.515073	0.522044	1.551788
O	-0.587130	-0.603888	-0.680919
C	-1.890709	-0.627624	-0.024815
H	-1.754803	-0.958039	1.006347
H	-2.475910	-1.366270	-0.571756
C	-2.510580	0.751279	-0.088786
H	-3.503104	0.726684	0.367009
H	-1.901844	1.467813	0.464115
H	-2.611971	1.081323	-1.124000
O	1.415342	-1.406439	-0.075524
H	0.191916	-1.498149	-0.579003

H	1.330492	1.241861	-1.432691
H	0.885550	2.547250	-0.300045
H	3.334143	2.065023	-0.150654
H	2.531117	1.621500	1.367959
H	2.986536	0.365204	0.190673
H	-3.048261	0.297737	-1.077180
H	-3.200546	-0.154510	0.688900
H	-2.075681	2.469716	-0.444721
H	-2.221447	2.013882	1.336055
H	-0.890145	1.205499	0.290795
C	0.591868	-1.790701	1.326233
H	-0.014483	-1.429328	2.157324
H	0.432819	-2.864589	1.210248
H	1.648045	-1.607074	1.524204

TS20

$E_{0K} = -764.3938422$ $ZPE = 0.1789160$

O	1.051656	-1.216193	-1.310082
P	0.098650	-0.987123	-0.207708
O	0.275702	0.688790	0.264461
O	-1.403716	-1.072996	-0.359403
C	1.272287	1.529081	-0.383513
C	2.612349	1.382682	0.305895
C	-2.769479	0.500156	-0.053955
C	-2.134861	1.685093	0.304499
